Photosynthesis Research (2020) 145:111–128
https://doi.org/10.1007/s11120-020-00762-7

ORIGINAL ARTICLE

The diversity and distribution of D1 proteins in cyanobacteria

Kevin J. Sheridan[1,2] · Elizabeth J. Duncan[3] · Julian J. Eaton-Rye[2] · Tina C. Summerfield[1]

Received: 30 December 2019 / Accepted: 25 May 2020 / Published online: 18 June 2020

Abstract

The *psbA* gene family in cyanobacteria encodes different forms of the D1 protein that is part of the Photosystem II reaction centre. We have identified a phylogenetically distinct D1 group that is intermediate between previously identified G3-D1 and G4-D1 proteins (Cardona et al. Mol Biol Evol 32:1310–1328, 2015). This new group contained two subgroups: $D1^{INT}$, which was frequently in the genomes of heterocystous cyanobacteria and $D1^{FR}$ that was part of the far-red light photoacclimation gene cluster of cyanobacteria. In addition, we have identified subgroups within G3, the micro-aerobically expressed D1 protein. There are amino acid changes associated with each of the subgroups that might affect the function of Photosystem II. We show a phylogenetically broad range of cyanobacteria have these D1 types, as well as the genes encoding the G2 protein and chlorophyll *f* synthase. We suggest identification of additional D1 isoforms and the presence of multiple D1 isoforms in phylogenetically diverse cyanobacteria supports the role of these proteins in conferring a selective advantage under specific conditions.

Keywords Cyanobacteria · D1 · Evolution · Photosystem II · Phylogenetics · *psbA*

Introduction

Photosystem II (PS II) catalyses the light-driven splitting of water at the start of the photosynthetic electron transport chain in the thylakoid membrane of oxygenic phototrophs (Vinyard and Brudvig 2018). High-resolution PS II structures (~ 1.9 to 2.1 Å) have been obtained from thermophilic cyanobacteria (Umena et al. 2011; Suga et al. 2015, 2017; Kern et al. 2018) and detailed structures confirming a high degree of conservation in eukaryotes have been obtained (Ago et al. 2016; Wei et al. 2016). The major polypeptides of the PS II reaction centre are referred to as D1 and D2 and these proteins provide the majority of the ligands to the redox active cofactors. In particular, the D1 protein provides the majority of the ligands to the Mn_4CaO_5 oxygen-evolving complex (OEC) with the remainder coming from the chlorophyll-binding CP43 protein of the core antenna (Ferreira et al. 2004; Shen 2015). Although D1 and D2 form a heterodimer, only the D1 branch is active in the reduction of the primary and secondary plastoquinone electron acceptors Q_A and Q_B (Cardona et al. 2012). In addition, the oxidative chemistry and photochemistry associated with water splitting results in light-induced photodamage that preferentially targets the D1 protein and subsequently D1 has a higher turnover rate than the other PS II proteins (Mulo et al. 2009).

Many cyanobacteria contain multiple copies of the *psbA* gene which encodes the D1 protein (Mulo et al. 2012), with some cyanobacteria containing as many as eight copies. A survey of 360 cyanobacterial D1 proteins supported the previous identification of several distinct types of the D1 protein (G0–G4), with the majority of cyanobacteria having between two and four isoforms encoded by three to six copies of *psbA* (Cardona et al. 2015). The G4 type (G4-D1) is the most prevalent form of D1 that supports oxygen evolution and this is the D1 type found in plants. It has been suggested that plastids evolved from an ancestor of extant cyanobacterium *Gloeomargarita lithophora* which has only *psbA* genes encoding the G4-D1 unlike the other deeply

Electronic supplementary material The online version of this article (https://doi.org/10.1007/s11120-020-00762-7) contains supplementary material, which is available to authorized users.

✉ Tina C. Summerfield
tina.summerfield@otago.ac.nz

[1] Department of Botany, University of Otago, Dunedin, New Zealand

[2] Department of Biochemistry, University of Otago, Dunedin, New Zealand

[3] Department of Biological Sciences, School of Biology, University of Leeds, Leeds, UK

branching cyanobacteria (Ponce-Toledo et al. 2017). All cyanobacteria investigated to date contain at least one gene encoding a G4-D1 and some strains contain multiple copies of *psbA* encoding G4-D1. Two variants of G4-D1 have been designated as D1:1 and D1:2 (Cardona et al. 2015). When environmental conditions result in increased turnover of D1, multiple copies of *psbA* encoding G4-D1 can benefit cyanobacteria in one of two ways. Firstly, the up-regulation of genes encoding identical copies of D1 (D1:1) increases both the *psbA* transcript pool and the D1 protein level, facilitating rapid replacement of photodamaged D1, thereby reducing photoinhibition (El Bissati and Kirilovsky 2001). In the second mechanism, the *psbA* gene encoding D1:2 is up-regulated. The alternative D1:2 copy is characterised by an amino acid substitution from glutamine to glutamate at position 130. This amino acid change decreases photoinhibition under high light by reducing the formation of triplet state chlorophyll species and singlet oxygen by favouring direct recombination (Vinyard et al. 2014). However, further amino acid differences between D1:1 and D1:2 appear to the impact PS II efficiency (Vinyard et al. 2014).

Evidence for additional roles of D1 proteins includes the up-regulation of a *psbA* gene under low-oxygen conditions in several cyanobacteria: *Synechocystis* sp. PCC 6803, *Thermosynechococcus elongatus* BP-1, *Cyanothece* sp. ATCC 51142 and *Anabaena* sp. PCC 7120 (Summerfield et al. 2008; Sicora et al. 2009). The D1´ proteins encoded by these low-oxygen-induced *psbA* genes share three amino acid substitutions, Gly80Ala, Phe158Leu and Thr286Ala (Sicora et al. 2009). Furthermore, PS II centres containing the D1´ in *Synechocystis* sp. PCC 6803 produced higher rates of oxygen than centres containing D1:1 from *psbA2* when expressed under the low-oxygen promoter (Crawford et al. 2016). A conserved role for these micro-aerobic D1´ proteins is supported by the finding that they were part of a monophyletic group of sequences (G3) from 39 cyanobacterial strains (Cardona et al. 2015).

Phylogenetic analysis of D1 proteins identified three groups lacking residues that provide ligands to the OEC (Cardona et al. 2015). One group (G2) contained 36 proteins (G2-D1), including the rogue D1 identified by Murray (2012), also named sentinel D1 by Wegener et al. (2015). The *psbA* gene encoding the G2-D1 from *Cyanothece* sp. ATCC 51142 was up-regulated in the subjective dark and it has been proposed that this copy of D1 is incorporated into inactive PS II centres to protect oxygen-sensitive enzymes such as nitrogenase (Toepel et al. 2008). Wegener et al. (2015) demonstrated that expression of the *psbA* gene encoding G2-D1 from *Cyanothece* sp. ATCC 51142 in *Synechocystis* sp. PCC 6803 resulted in inactive PS II centres when G2-D1 was present. In the unicellular diazotroph *Crocosphaera watsonii* WH8501, during the dark period, G2-D1-containing PS II centres were detected in low numbers consistent with a regulatory role (Masuda et al. 2018). Signalling from the small numbers of G2-D1 PS II centres was part of a proposed two-step mechanism for the inactivation of PS II to protect nitrogenase activity in *Cyanothece* sp. ATCC 51142 (Sicora et al. 2019).

The second phylogenetic group of D1 proteins lacking ligands to the OEC (designated as G1 in Cardona et al. 2015) contained the super rogue class of D1 reported by Murray (2012), and this isoform has subsequently been identified as a chlorophyll *f* synthase that catalyses the production of a far-red/near-infrared absorbing chlorophyll *f* (Ho et al. 2016). The chlorophyll *f* synthase gene is in a far-red-inducible gene cluster (FaRLiP) that is up-regulated under prolonged exposure to far-red/near-infrared wavelengths of light. Genes in this cluster encode alternative Photosystem I (PS I), PS II and phycobilisome proteins, along with regulatory proteins, that modify the photosynthetic electron transport chain as a part of a far-red photoacclimation process (Gan et al. 2014; Ho et al. 2016; Nürnberg et al. 2018; Shen et al. 2019). The final phylogenetic group of D1, G0, contained a single sequence from *Gloeobacter kilaueensis* JS1 (Cardona et al. 2015). This sequence also lacks the ligands to bind the OEC, having a C-terminus which is more similar to D2 than D1 and has an unknown function.

To further investigate the possible roles and extent of D1 diversity in cyanobacteria, we expanded the phylogenetic analyses of D1 proteins using 206 cyanobacterial genomes. We have identified two additional phylogenetically distinct groups of D1 proteins and identified distinct subgroups within the G3-D1 sequences. Our approach has shown the distribution of *psbA* genes is highly varied among the cyanobacteria, likely reflecting particular *psbA* combinations associated with cyanobacteria found in different microhabitats.

Methods

Phylogenetic analysis

A total of 206 cyanobacterial genomes and the G0, 16S and 23S rRNA sequences for *Gloeobacter kilaueensis* JS1 were retrieved from JGI (Grigoriev et al. 2012; Nordberg et al. 2014) and NCBI (Benson et al. 2017) from the 3rd to 7th of January, 2017 and 796 *psbA* gene sequences were extracted from these genomes. The minimum length criteria for inclusion in analyses was approximately two-thirds of the entire sequence (600 bp minimum sequence length). The 16S–23S rRNA (ribosomal RNA) gene sequences were retrieved from the same database as the *psbA* genes with the exception of *Leptolyngbya* sp. JSC-1 for which these data were unavailable. In this case, a partial 16S rRNA gene copy was retrieved from the SILVA ribosomal RNA database (Quast et al. 2013).

Phylogenetic analyses of D1 sequences were performed using the same approach as Cardona et al. (2015) using the atypical sequence from *Gloeobacter kilaueensis* JS1 (G0), described by Saw et al. (2013) as the outgroup. Briefly, the D1 phylogeny was constructed in PhyML using the LG model of amino acid substitution, four gamma rate categories and the nearest neighbour interchange method for tree improvement. All other parameters were left as default, with the software allowed to estimate the equilibrium frequencies, proportion of invariant sites and the gamma-shaped parameter. Branch supports were calculated using the SH-like approximate likelihood ratio test option (Shimodaira and Hasegawa 1999) with branch supports above 0.85 (85%) being used as the cutoff threshold. The creation of multiple sequence alignments was aided by generating PDB files for a representative D1 sequence from each D1 protein group using the SWISS-MODEL online service from ExPasy (Guex et al. 2009; Bertoni et al. 2017; Bienert et al. 2017; Waterhouse et al. 2018). The PDB file creation utilised the crystal structure from *Thermosynechococcus vulcanus* (4UB6) as reference (Suga et al. 2015). The resulting PDB files were then aligned using the CE align function (Shindyalov and Bourne 1998) in PyMOL (DeLano 2002, 2009) and used in the creation of PyMOL figures. Pairwise alignments of all G3 sequences, as well as the $D1^{INT}$ and $D1^{FR}$ found in this analysis, were also conducted.

A species tree of the 206 cyanobacterial strains, along with the outgroup, was created based on rRNA gene sequences. Briefly, the 16S and 23S rRNA gene sequences were concatenated and aligned using the default parameters of ClustalW (Larkin et al. 2007) and manually checked. As rRNA gene sequences cannot always definitively discriminate between two closely related species (Jaspers and Overmann, 2004), SNPs within multiple copies of the 16S or 23S rRNA gene sequence were utilised to assist in discrimination (Hakovirta et al. 2016). This was achieved by taking the consensus sequence to build the 16S–23S rRNA species tree. In accordance with Hilton et al. (2016) only those alignment sites which had at least 90% coverage were used in the subsequent phylogenetic analysis (Felsenstein 1985). The best-fit model of nucleotide substitution was determined using the JmodelTest 2.1 to generate both the maximum likelihood RAxML and maximum parsimony (PAUP) trees, respectively (Swofford 2001; Stamatakis 2006; Darriba et al. 2012). The data were analysed in both cases using generalised time reversible (GTR) + Γ + I. The most parsimonious trees were found following 1000 replicate heuristic searches with 100 trees saved per replicate to produce a maximum of 10,000 trees. The branch support was then calculated using bootstrap of 1000 replicates. The bootstrap values from the maximum parsimony analysis were transferred to the corresponding branches of the maximum likelihood tree. The maximum likelihood tree was found using 1000 bootstrap iterations. Bootstrap support over 0.95 was used as the threshold cutoff.

Identification of genes under purifying selective pressure

Pairwise comparison estimates of rates of synonymous (dS) and non-synonymous substitutions (dN) were calculated using codeML in the graphical interface for PAML, PAMLX (Yang 2007; Xu and Yang 2013). Estimates of the ratio of non-synonymous to synonymous mutations, ω (dN/dS), was used to investigate whether each subgroup of *psbA* homologs encoding mature D1 protein sequences were undergoing patterns of neutral drift ($\omega = 1$), purifying selection ($\omega < 1$) or positive selection ($\omega > 1$). The nucleotide multiple sequence alignment of the *psbA* genes encoding each group of D1 proteins was built using the protein alignment for reference. In accordance with Fletcher and Yang (2010), gaps and uncertainties within the multiple sequence alignment were stripped from the alignment to avoid false positives. Additionally, identical nucleotide sequences present in single cyanobacterial strains were also removed to avoid spurious replication of data (Hongo et al. 2015). The *rbcL* gene from all strains was included as a reference in this analysis, this gene encodes the large subunit of ribulose-1,5-bisphosphate carboxylase/oxygenase (Rubisco).

Results and discussion

Diversity of the D1 protein family

The analysis of the D1 protein family used in this study employed the LG model of amino acid substitution (Le and Gascuel 2008). This accounts for among-site rate variation and provides replacement rate estimates using rescaling of amino acid changes observed in the data depending on whether they occur in slow or fast sites. It should be noted that this model is based on a large, diverse data set to estimate a general replacement matrix rather than a more specific matrix. The maximum likelihood phylogeny of D1 proteins (Figs. 1 and S1) generated using D1 sequences from 206 cyanobacterial strains and the G0 sequence from *Gloeobacter kilaueensis* JS1 showed a similar structure to the previously reported work of Cardona and colleagues with the grouping of D1 proteins not following cyanobacterial phylogenies (Cardona et al. 2015; Grim and Dick 2016). The G0-D1 sequence from *Gloeobacter kilaueensis* JS1 currently has no identified function, and has been suggested to represent the most ancestral D1 sequence based on its position in the type II reaction centre phylogeny of Cardona et al. (2019). Both the amino acid and nucleotide sequences for this purported ancestral D1 have been used as the outgroup

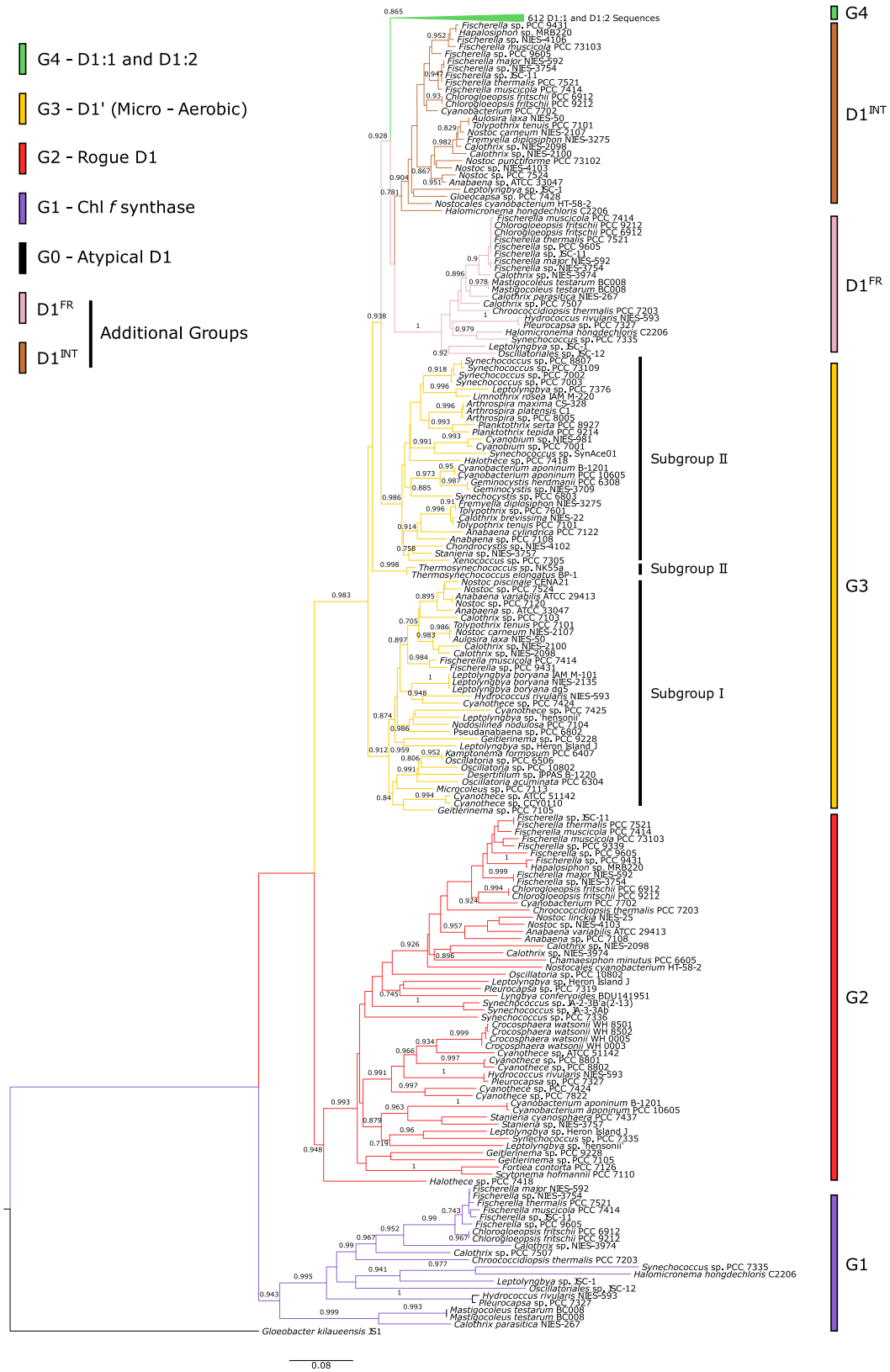

Fig. 1 Rooted maximum likelihood phylogeny of D1 proteins using the atypical D1 from *Gloeobacter kilaueensis* JS1 as the outgroup. Branch supports are expressed as SH-like aLRT probabilities. The G0 sequence from *Gloeobacter kilaueensis* JS1 is coloured in black, with G1, G2, G3 and G4 D1 proteins shown in purple, red, yellow and green, respectively. The two D1 protein groups: $D1^{FR}$ and $D1^{INT}$ are indicated in pink and brown, respectively

in previous phylogenetic studies (Cardona et al. 2015; Grim and Dick 2016). The largest D1 group corresponded to the G4 of Cardona et al. (2015) and this contained 612 of the 796 sequences; including the well-characterised proteins from *Synechocystis* sp. PCC 6803 (D1:1) and *Thermosynechococcus elongatus* BP-1 (both D1:1 and D1:2 proteins) (Figs. 1 and S1, shown in green).

Sister to G4 was a group that contained two D1 subgroups, one with moderate support and one well supported (Fig. 1). This group represents an expansion of the intermediate group of Cardona et al. (2015) from 9 to 47 sequences (Figs. 1 and S1; subgroups shown in pink and brown). One subgroup contained 27 D1 sequences, this group will be referred to as $D1^{INT}$ (INT for 'intermediate' as no current function has been ascribed to this group and on the phylogenetic tree these sequences are intermediate between G3 and G4). The second subgroup contained 20 D1 sequences and strains containing these sequences have been shown to contain the FaRLiP gene cluster (Gan et al. 2015). This group will be hereafter referred to as $D1^{FR}$ (FR for far-red).

The next group corresponding to the G3 category from Cardona et al. (2015), which contained the micro-aerobically induced D1′, had increased from 39 to 64 sequences, with almost a third of the analysed cyanobacteria having a *psbA* gene encoding G3-D1. The G3 sequences formed three well-supported subgroups (Figs. 1 and S1, shown in yellow-orange). Groups corresponding to G2 and G1 of Cardona et al. (2015) were also resolved. The G2 category was increased from 36 to 52 sequences (Figs. 1 and S1; shown in red), with genes encoding G2-D1 in approximately a quarter of cyanobacteria analysed. The G1 category was increased from 8 to 20 D1 proteins (Figs. 1 and S1; shown in purple). An alignment of consensus sequences for each D1 type is shown in Fig. 2 at 95% consensus and Fig. S2 for 50% consensus.

A phylogenetically distinct group of D1 protein sequences, $D1^{INT}$

All 27 $D1^{INT}$ sequences have two conserved amino acid changes compared to the G4 proteins: Tyr126 to Trp and Phe260 to Trp. In addition, there are four conserved residues in at least 85% of the $D1^{INT}$ sequences that occur in less than 5% of G4 sequences: Ala68 to Ser, Ser79 to Thr, Ser85 to Thr, Ala156 to Ser (Fig. 3a; and for full-length alignment, see Fig. S3). The residues Ser68, Thr79 and Thr85 are located in the lumenal ab-loop. The Tyr126 to Trp substitution is in helix B (Fig. 3b, c) and may directly affect active branch pheophytin ($Pheo_{D1}$) through the loss of the hydrogen bond to the 13^3-ester C=O of $Pheo_{D1}$ (Zabelin et al. 2014). On the other side of $Pheo_{D1}$, in helix C, the Ala156 to Ser substitution may alter hydrogen bonding to both Ala152 and Tyr161. The alanine at position 152 is thought to interact with the Phe435 of CP43, potentially modulating interactions between D1 and CP43 in the vicinity of $Pheo_{D1}$ (Fig. 3d, e) which Vinyard et al. (2014) suggest may alter the midpoint potential of this pheophytin. The alteration of the Phe260 to Trp is predicted, using in silico modelling, to open a hydrogen bond to the nearby phosphatidylglycerol (PG), a constitutive lipid within the PS II structure (Fig. 3f, g; and see Wada and Murata (2007) and Endo et al. (2019)) and studies by Narusaka et al. (1996, 1999) have suggested that this residue may be involved in phototolerance.

The majority of $D1^{INT}$ encoding genes were in diazotrophic cyanobacteria (25/27) and most of these cyanobacteria were heterocystous (24/27), this represented approximately one-third of the heterocystous cyanobacteria analysed in this study (24/71 heterocystous strains). To date specific conditions inducing the up-regulation of $D1^{INT}$ have not been identified.

The D1 proteins associated with the far-red light photoacclimation (FaRLiP) cluster

The 20 sequences belonging to the $D1^{FR}$ group in Fig. 1 are encoded by *psbA* genes in the far-red-inducible gene cluster described by Gan et al. (2014, 2015). This gene cluster has been identified in multiple cyanobacterial strains including *Calothrix* sp. PCC 7507, *Chlorogloeopsis fritschii* PCC 9212, *Chroococcidiopsis thermalis* PCC 7203, *Fischerella thermalis* PCC 7521, *Halomicronema hongdechloris* C2206 and *Synechococcus* sp. PCC 7335 (Nürnberg et al. 2018; Partensky et al. 2018; Ho and Bryant 2019; Ho et al. 2019; Chen et al. 2012, 2019). The gene cluster was shown to contain several genes encoding isoforms of PS II, PS I and phycobilisome proteins as well as regulatory genes. The far-red-inducible PS II genes include two annotated as *psbA*—one encoding chlorophyll *f* synthase and the other encoding $D1^{FR}$ (Gan et al. 2014, 2015). Our analysis supports the conclusion that all genes encoding $D1^{FR}$ are in a putative FaRLiP cluster (Fig. 4a; for gene context of the 20 *psbA* genes encoding $D1^{FR}$ in far-red-inducible gene clusters, see Fig. S4).

The $D1^{FR}$ proteins retain the essential ligands for binding the OEC. There were 16 conserved changes in the $D1^{FR}$ sequences compared to the 95% consensus of the G4 proteins, as well as three additional changes in which the $D1^{FR}$ proteins had one of two residues that differed from the G4-D1 residues at those positions. The majority of the altered residues are in the first three helices (for consensus, see Fig. 2 and full alignment, see Fig. S5). Within helix A, these proteins share deletion of a frequently observed Thr at position 40, and an insertion of Val before a conserved Phe and a characteristic Gly-Val-Ser motif between residues 43 and 45 (Fig. 4b). These residues occur in the vicinity of the bound ß-carotene and the accessory chlorophyll, Chl_{zD1},

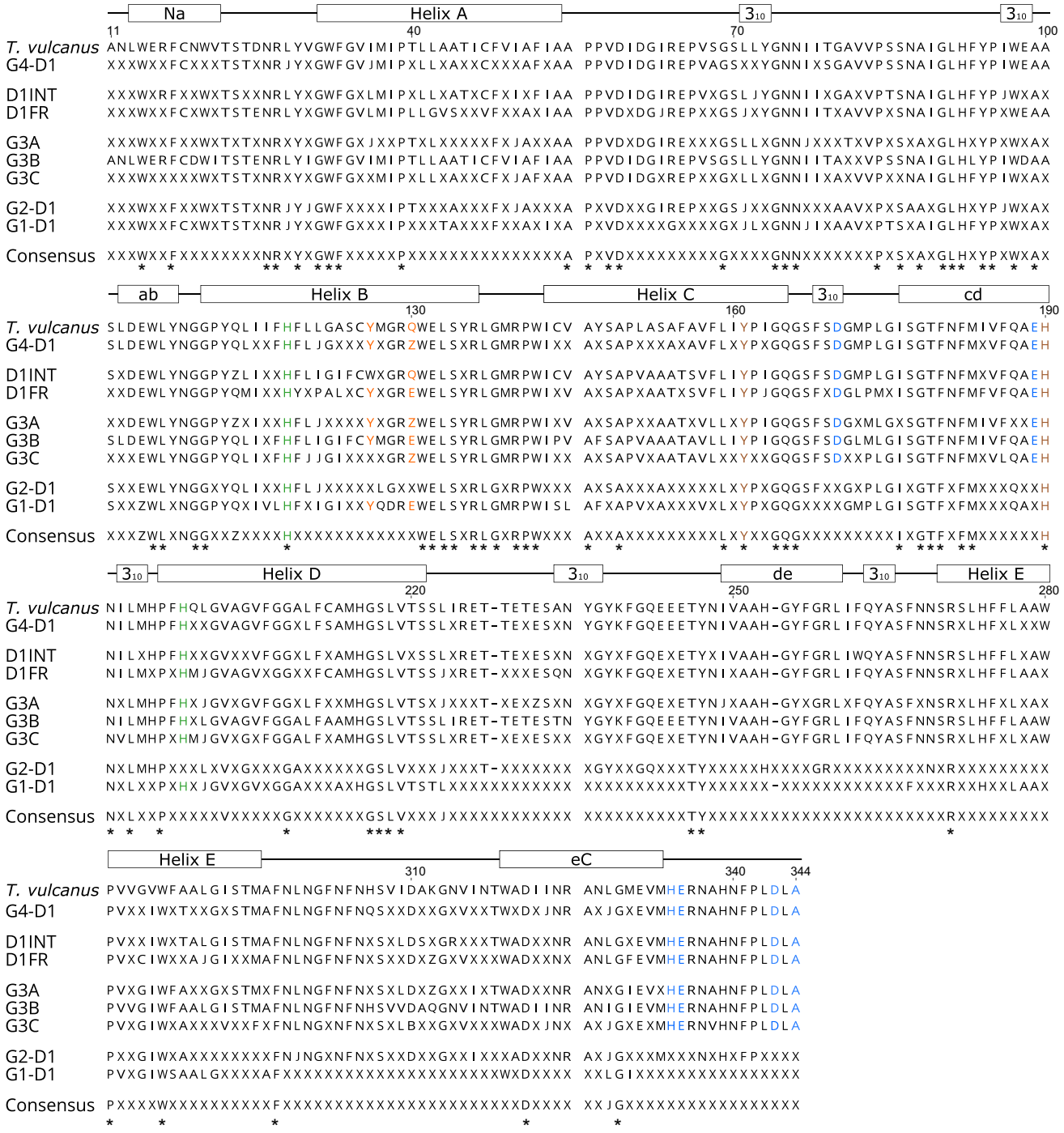

Fig. 2 Alignment of the 95% consensus for each group of D1 in the phylogenetic tree in Fig. 1 with a sequence representing the consensus for all eight D1 groups and the G4 sequence from *Thermosynechococcus vulcanus*. Positions highlighted with an asterisk indicate residues which are fully conserved across all types of D1. Ligands to the OEC, chlorophyll, Y_z and pheophytin are highlighted in blue, green, brown and orange, respectively. Helix annotation is based on https://www.rcsb.org/pdb/explore/remediatedSequence.do?structureId=4UB6, 310h indicates 310 helices

that might serve as side-path electron donors in PS II under specific conditions (Cardona et al. 2012). Between helices A and B there is a Ser79 to Thr change also found in the $D1^{INT}$ sequences.

In the $D1^{FR}$ protein helix B, the His118 ligand of Chl_{zD1} and the putative Tyr126 ligand of $Pheo_{D1}$ are unaltered; however, several residues are altered between Leu114 and Val/Ile/Cys123 which may modify the properties of these

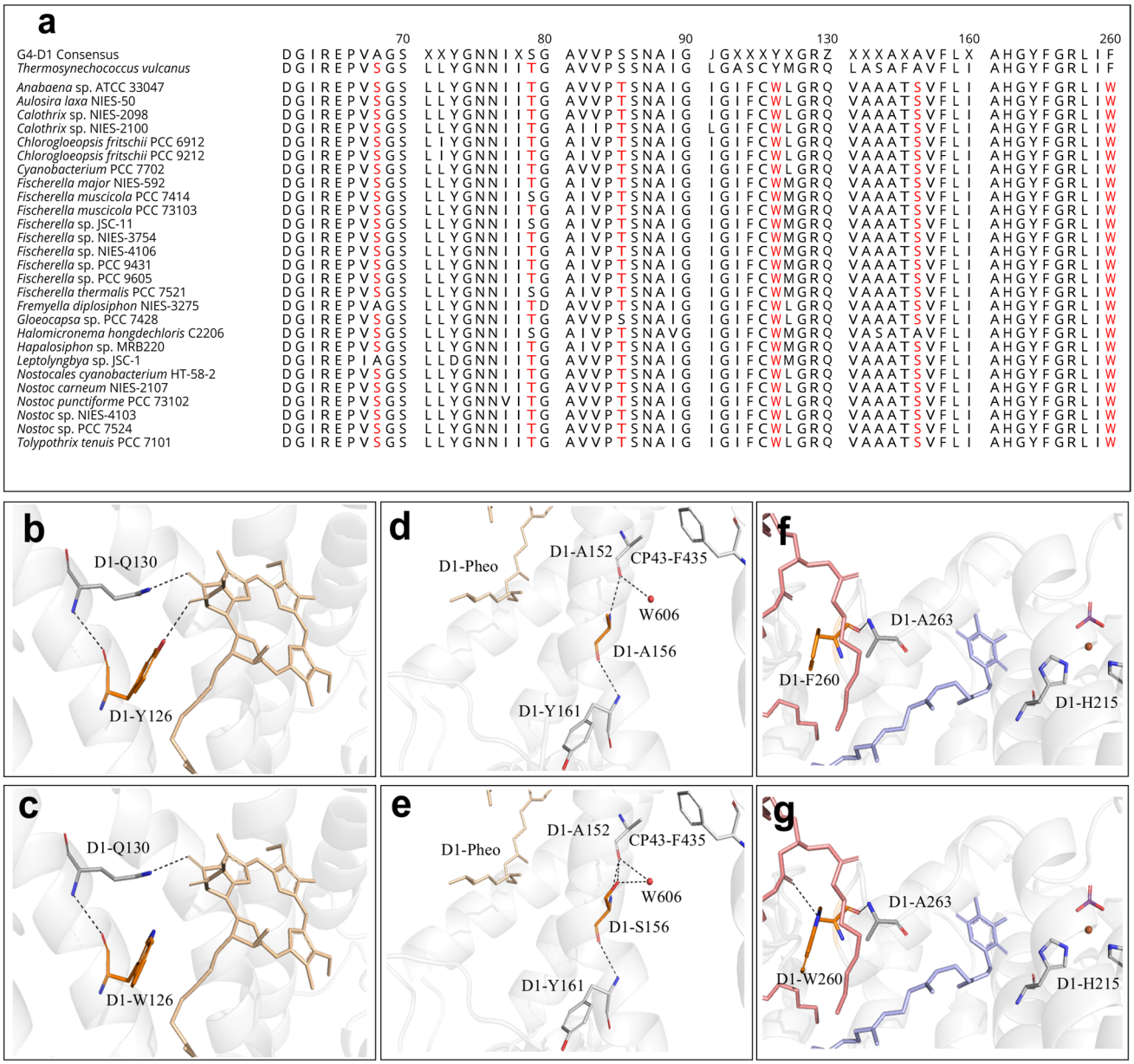

Fig. 3 Alignment of D1^{INT} sequences with conserved residues highlighted. **a** Alignment of D1^{INT} protein sequences compared to the G4 sequence from *Thermosynechococcus vulcanus* and the consensus sequence for G4-D1s, with conserved changes to the protein sequences highlighted in red. **b, d** and **f** show the structure of *Thermosynechococcus vulcanus* at Tyr126, 156 and Phe260, while **c, e** and **g** show the same residues as modelled for the D1^{INT} protein sequence from *Nostoc punctiforme* ATCC 29133. Distances within 3.6 Å, indicating potential hydrogen bonds are shown in dashed, black lines. The pheophytin present in the D1 protein is shown in tan. Q_B is shown in blue. The phosphatidylglycerol adjacent to Phe260 is shown in salmon pink in **f** and **g**

cofactors (Fig. 4c, d). The D1^{FR} sequences usually contain the substitution of Gln to Glu at position 130 which is characteristic of the G4 high-light form, D1:2. In addition, the D1^{FR} sequences have the Ala156 to Ser change observed in the D1^{INT} but Ala154 is changed to a Thr in this group which may further modify the efficiency of charge recombination (Fig. 4e, f) (Vinyard et al. 2014). It has been suggested that Thr154 and Tyr119 (instead of Phe) of D1^{FR} may also have a hydrogen bond to the formyl group of chlorophyll *f* (Nürnberg et al. 2018). Between helices C and D, the D1^{FR} Met172 to Leu and Leu174 to Met changes are found; these are located in a region separating the Mn_4CaO_5 cluster from Chl_{zD1} and P_{D1} of P680 (Kern et al. 2007). A Phe184 change is also found in this region in D1^{FR} sequences while in helix D there is a Ser212 to Cys change (Fig. 4b).

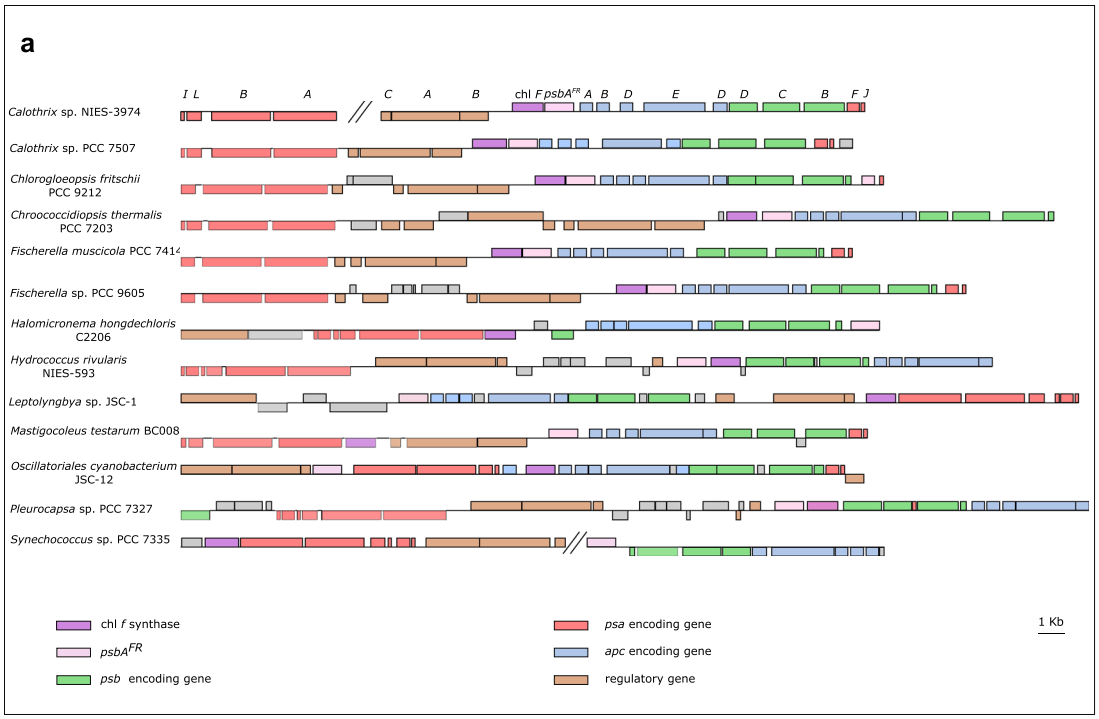
a
I L B A C A B chl f psbA^FR A B D E D D C B F J
Calothrix sp. NIES-3974
Calothrix sp. PCC 7507
Chlorogloeopsis fritschii PCC 9212
Chroococcidiopsis thermalis PCC 7203
Fischerella muscicola PCC 7414
Fischerella sp. PCC 9605
Halomicronema hongdechloris C2206
Hydrococcus rivularis NIES-593
Leptolyngbya sp. JSC-1
Mastigocoleus testarum BC008
Oscillatoriales cyanobacterium JSC-12
Pleurocapsa sp. PCC 7327
Synechococcus sp. PCC 7335
chl f synthase
psbA^FR
psb encoding gene
psa encoding gene
apc encoding gene
regulatory gene
1 Kb

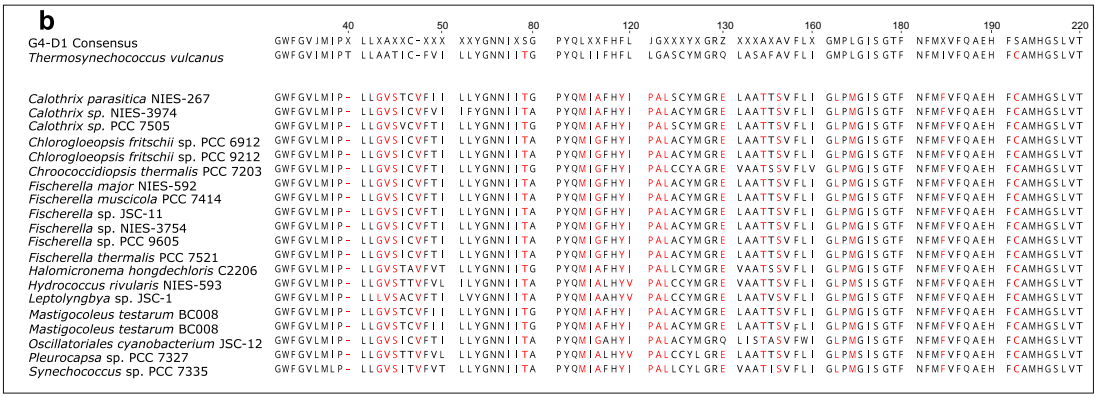
b
G4-D1 Consensus
Thermosynechococcus vulcanus
Calothrix parasitica NIES-267
Calothrix sp. NIES-3974
Calothrix sp. PCC 7505
Chlorogloeopsis fritschii sp. PCC 6912
Chlorogloeopsis fritschii sp. PCC 9212
Chroococcidiopsis thermalis PCC 7203
Fischerella major NIES-592
Fischerella muscicola PCC 7414
Fischerella sp. JSC-11
Fischerella sp. NIES-3754
Fischerella sp. PCC 9605
Fischerella thermalis PCC 7521
Halomicronema hongdechloris C2206
Hydrococcus rivularis NIES-593
Leptolyngbya sp. JSC-1
Mastigocoleus testarum BC008
Mastigocoleus testarum BC008
Oscillatoriales cyanobacterium JSC-12
Pleurocapsa sp. PCC 7327
Synechococcus sp. PCC 7335

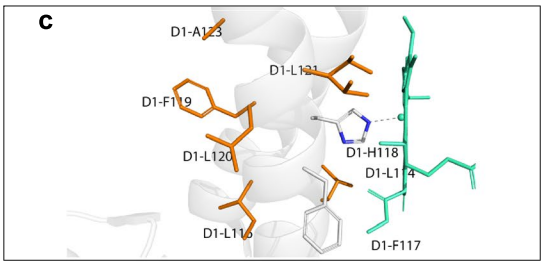
c
D1-A123
D1-L121
D1-F119
D1-H118
D1-L120
D1-L114
D1-L116
D1-F117

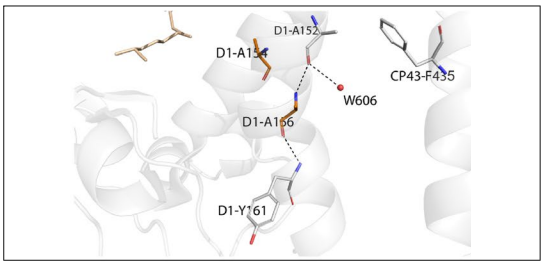
D1-A152
D1-A154
CP43-F435
W606
D1-A156
D1-Y161

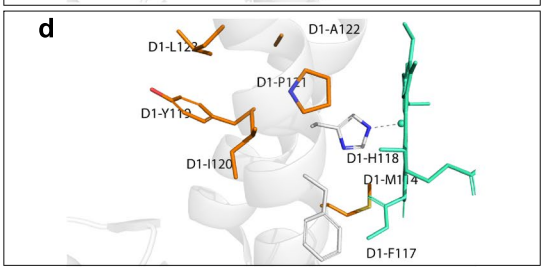
d
D1-L123
D1-A122
D1-P121
D1-Y119
D1-I120
D1-H118
D1-M114
D1-F117

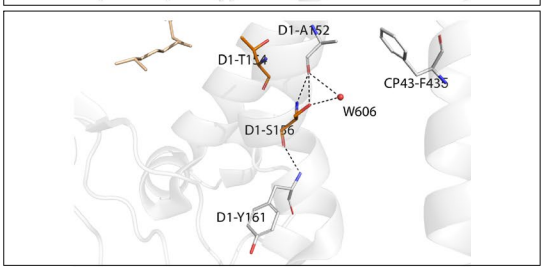
D1-A152
D1-T154
CP43-F435
W606
D1-S156
D1-Y161

◂**Fig. 4** Gene context, sequence alignment and highlighted residues of interest for $D1^{FR}$ sequences. **a** Gene context of the chlorophyll *f* synthase and $D1^{FR}$ in the far-red-inducible gene cluster. Identity of the genes present in the *Calothrix* sp. NIES-3974 are given for reference. **b** Alignment of the 20 $D1^{FR}$ sequences with the reference G4 sequence from *Thermosynechococcus vulcanus* and the consensus sequence for all G4-D1s; conserved modified residues in $D1^{FR}$ highlighted in red. **c** and **d** The D1 helix B residues present in the *Thermosynechococcus vulcanus* PS II crystal structure and the same region present in the $D1^{FR}$ sequence from *Chlorogloeopsis fritschii* PCC 9212, respectively. **e** and **f** D1 helix C from the PS II structure from *Thermosynechococcus vulcanus* and the corresponding region for the modelled D1 from *C. fritschii* PCC 9212, respectively. In **c** and **d** the accessory chlorophyll in PS II is shown in cyan, while the pheophytin in **e** and **f** is shown in tan

Ho et al. (2016) and Shen et al. (2019) showed that the G1-D1 is required for the production of chlorophyll *f*. A G1-*psbA* null mutant abolished chlorophyll *f* production in both *Chlorogloeopsis fritschii* PCC 9212 and *Synechococcus* sp. PCC 7335, while chlorophyll *f* could be produced in far-red light in the non-FaRLiP strain, *Synechococcus* sp. PCC 7002, when this strain contained a G1-encoding *psbA* gene. Chlorophyll *f* is present in the reaction centres of both PS II and PS I (Ho et al. 2016; Nürnberg et al. 2018; Shen et al. 2019). In studies using isolated PS II centres of *Chroococcidiopsis thermalis* PCC 7202, the isolated PS II appeared to contain the $D1^{FR}$ protein when subjected to far-red light (Nürnberg et al. 2018).

The G3 D1 group contains multiple subgroups

The D1 phylogeny divided the G3 proteins into three well-supported subgroups (SH-like aLRT > 0.9). Each subgroup contained proteins encoded by *psbA* genes that are up-regulated under micro-aerobic conditions (Summerfield et al. 2008; Sicora et al. 2009) (Figs. 1 and S1); these were *Nostoc* sp. PCC 7120 and *Cyanothece* sp. ATCC 51142 in subgroup I, *Thermosynechococcus elongatus* BP-1 in subgroup II and *Synechocystis* sp. PCC 6803 in subgroup III. The separation of G3-D1 into these subgroups was also observed when these 64 sequences were analysed using the original outgroup or a representative sequence from each of the other D1 groups to root the tree (Figs. S6–S9). The G3 subgroups contain 33, 2 and 29 sequences, respectively (Fig. 1). The two main subgroups have alterations in the amino acids that frequently contribute to the secondary ligand sphere of the OEC (highlighted in Fig. 5; for full alignment of G3 protein sequences see Fig. S10 and Table S1).

The three characteristic amino acid changes of low-oxygen-induced *psbA* encoded proteins identified by Sicora et al. (2009) (Gly80 to Ala, Phe158 to Leu and Thr286 to "Ala") were in 61 of the 64 protein sequences in G3. However, the Gly80 to Ala substitution was not in the G3 protein sequence from *Oscillatoria* sp. PCC 6506 or *Kamptonema formosum* PCC 6407 in subgroup I. All G3 sequences contained the Phe158 to Leu change, but the *Geitlerinema* sp. PCC 7105 subgroup I sequence did not have the Thr286 to Ala change (Figs. 5 and S10).

In subgroup I, residues that differed to the 95% G4 consensus sequence in at least 90% of the sequences included Leu41 to Ala (rarely Ile or Gly), Cys47 to Val (rarely Ala or Thr) both in helix A, and in the a-b loop, both Ala81 to Thr and Ser85 to Thr. The Asn87 residue is replaced with an Ala in almost 80% of the subgroup I sequences; this Asn has been reported to interact with a chloride-binding site associated with a proton exit channel for the OEC (Banerjee et al. 2018, 2019). In addition, Asn87 may also interact with CP43-Glu354 and CP43-Arg357 through hydrogen bonding but these interactions would in all likelihood be lost when the residue is Ala (Fig. 5b, c). Also in subgroup I (and subgroup II) a Pro to Met change is observed at position 173 in the c-d loop; this substitution in *T. elongatus* has been shown to affect oxidation of the redox active Tyr161 (Y_Z) and weaken the hydrogen bond between Y_Z and His190 (Sugiura et al. 2014).

In subgroup III, residues that differed to the 95% G4 protein consensus sequence are more frequently found between helix C and the C-terminus. Residues changed with respect to the G4 sequence that are characteristic of this G3 subgroup include Pro162 to Ser (rarely Ala, in helix C), Phe186 to Leu in helix CD in the c-d loop, Ile192 to Val (also found in the c-d loop of 8 out of 33 subgroup I sequences), as well as, Thr292 to Cys or Ser and Met293 to Phe in helix E and Ala336 to Val (Fig. 2).

Introduction of the Pro162 to Ser change found in D1´ in *Synechocystis* sp. PCC 6803 did not alter oxygen evolution; however, the F186L and F186L:P162S mutants exhibited perturbed oxygen evolution and Q_A to Q_B electron transfer (Funk et al. 2001; Wiklund et al. 2001; Sicora et al. 2004). Phe186 is hydrogen bonded to His190 and Phe182 as part of a putative hydrogen bond network involving several bound waters in the vicinity of Y_Z (Fig. 5d, e). Both Phe186 and Phe182 along with Met293 contribute to a hydrophobic pocket, as previously noted, separating the OEC from P680 (Kern et al. 2007). The Met-to-Phe substitution at position 293 likely disrupts hydrogen bonding involving Asn296 and potentially Gln165. Asn296 and Gln165 of G4 are hydrogen bonded to oxygen atoms which interact with the OEC.

The Ile at position 192 in G4 that becomes a Val in G3 subgroup III is located on the lumenal side of the D1 protein, while no specific role for this residue could be ascertained in silico, a I192F:N267I double mutant in *Synechocystis* sp. PCC 6803 prevented photoautotrophic growth (Yamasato et al. 2002). The G4 Ala336 position that is a Val in subgroup III is likely to interact with the OEC ligand, His337, and may interact with Asp61, which binds the OEC through a water molecule (W567 in PDB 4UB6) (Fig. 5f, g).

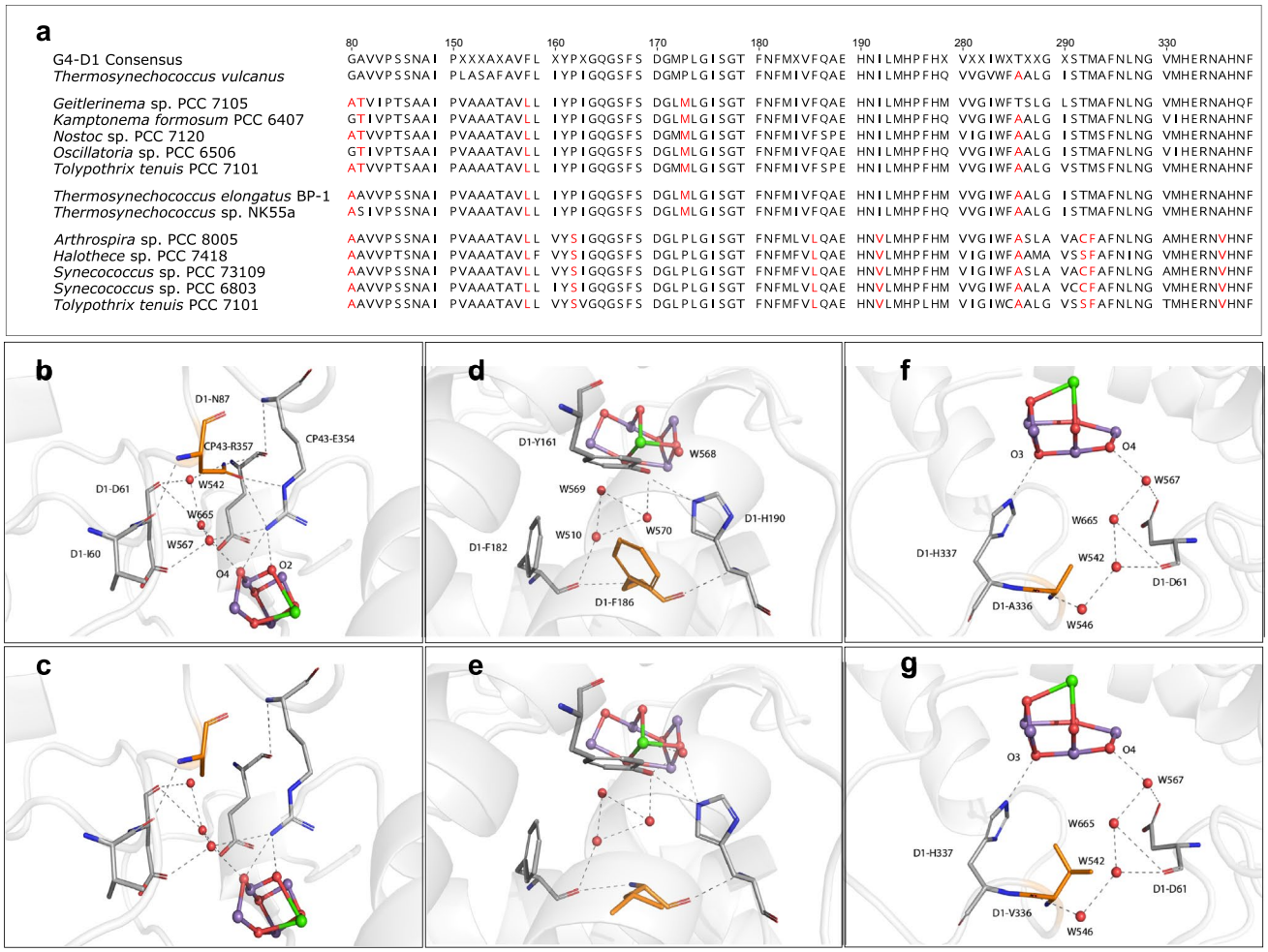

Fig. 5 Alignment of all sequences and highlighted residues of interest for G3-D1 sequences. **a** Alignment of five subgroup I D1´ sequences (*Geitlerinema* sp. PCC 7105–*Tolypothrix tenuis* PCC 7101, two subgroup II sequences (*Thermosynechococcus elongatus* BP-1 and *Thermosynechococcus* sp. NK55a) and five subgroup III sequences (*Arthrospira* sp. PCC 8005–*Tolypothrix tenuis* PCC 7101) against the G4 reference sequence from *Thermosynechococcus vulcanus* and the consensus sequence for all G4-D1 sequences with subgroup-specific alterations to the D1 protein structure highlighted in red. **b** and **c** comparison of the amino acids around Asn87 in the *Thermosynechococcus vulcanus* PS II crystal structure and the modelled Ala87 from the G3-D1 protein of *Nostoc* sp. PCC 7120. **d**,**e**,**f** and **g** show the interactions of Phe186 and Ala336 of the G4-D1 from the *Thermosynechococcus vulcanus* PS II crystal structure and the modelled alterations of these ligands from the G3-D1 protein of *Synechocystis* sp. PCC 6803, respectively. Both G3-D1 sequences from *Nostoc* sp. PCC 7120 and *Synechocystis* sp. PCC 6803 were modelled based on the known crystal structure of D1 from *Thermosynechococcus vulcanus* as described in methods. The potential hydrogen-bonding network surrounding these residues is shown in dashed, black lines and limited to distances within 3.6 Å. The OEC is shown in balls and sticks with the calcium, manganese and oxygen shown in green, purple and red, respectively

The G1 and G2 D1 proteins

The G2 of Cardona et al. (2015) included the rogue and sentinel D1s described by Murray (2012) and Wegener et al. (2015), respectively, these lack a number of key amino acids required to support normal PS II function. In our extended analysis, 52 G2-D1 proteins were identified: the additional sequences had the same donor and acceptor side changes reported previously (Cardona et al. 2015) (Fig. 2) but three residues were no longer conserved across all the G2 members (Glu65, His252 and Gly256).

In agreement with previous reports, none of the G2 members have the 341–344 Leu-Asp-Leu-Ala motif that is conserved in G4, $D1^{INT}$, $D1^{FR}$ and G3 (except one G3-D1 with a Leu341to Met change) on the N-terminal side of the CtpA cleavage site. The C-terminus was altered in four G2-D1 sequences from unicellular strains (*Cyanobacterium aponinum* strains and *Stanieria* spp.), these ended at position 343, in addition, 23 G2 sequences had an Ala344 to Ser change. The remainder of the strains (25) had Ala at position 344 with the number of amino acids following this residue varying from zero to 27 amino acids. This sequence variation

in G2-D1 would be consistent with no processing of the C-terminus suggested by Wegener et al. (2015).

The G1 group of Cardona et al. (2015) contained eight protein sequences of the far-red-inducible chlorophyll *f* synthase, which catalyses the production of chlorophyll *f* (Chen et al. 2010) and was first identified by Murray (2012). The ligands necessary to bind the OEC, which are provided by Asp170, Glu189, His332, Glu333, Asp342 and Ala344 were absent or not conserved in the G1 category of proteins as previously reported by Cardona et al. (2015). The G1 sequences did retain other ligands necessary to bind PS II cofactors, e.g. His118 which provides the axial ligand to the accessory chlorophyll *a* (Chl_{zD1}), the residues binding pheophytin ($Pheo_{D1}$) at positions Thr126 and Glu130 and the axial ligand at His198 for the reaction centre chlorophyll P_{D1}, as well as the key Tyr161 (Yz) and His190 pairing on the donor side. However, the G1 sequences contain substitutions around the Chl_{zD1} binding site with all sequences having changes Ile116 to Val, Phe117 to Leu, Leu121 to Ile and Ala123 to Ile. In the vicinity of the $Pheo_{D1}$ binding site, the G1 sequences included the changes Met127 to Gln and Gly128 to Asp (Fig. 2).

Purifying selection pressure within the *psbA* genes encoding the D1 protein family

The *psbA* genes encoding all the different D1 protein sequences are subject to similar, relatively strong, purifying selection; this was similar to that observed for the gene *rbcL* that encodes the Rubisco large subunit (Fig. 6). Of the seven groups, the G1 sequences exhibited slightly more relaxed selection (mean $\omega = 0.071 \pm 0.045$). Genes encoding the $D1^{FR}$ and $D1^{INT}$ proteins were found to be undergoing the highest amount of purifying selection (mean $\omega = 0.020 \pm 0.013$ and mean $\omega = 0.026 \pm 0.003$, respectively). This may indicate that amino acid changes in the mature D1 protein of all the D1 isoforms can either impair or retard the performance of PS II, suggesting that this protein family is retaining amino acids critical to their function: indicating that all of these proteins are likely to be physiologically relevant (Fig. 6).

Distribution of the *psbA* genes encoding the D1 protein family in cyanobacteria

The 16S–23S rRNA gene phylogeny shows the relationship of the 206 cyanobacterial strains used in this study. This phylogeny has been annotated with the type of D1 proteins found in each strain along with the number of genes encoding each type of D1 (Fig. 7). The cyanobacterial clades recovered in this analysis were compared to the previous analysis of Shih et al. (2013) (Fig. 7). While the two analyses differed in that the analysis of Shih et al. (2013) used 31 concatenated protein sequences to generate the species tree, both approaches produced similar cyanobacterial groupings and therefore the clade annotation used in Fig. 7 is the same as that used in Shih et al. (2013). All cyanobacterial genomes examined contain at least one copy of a *psbA* gene encoding G4-D1 (either a D1:1 or D1:2 or both). It should be noted that this analysis includes draft genomes and in some

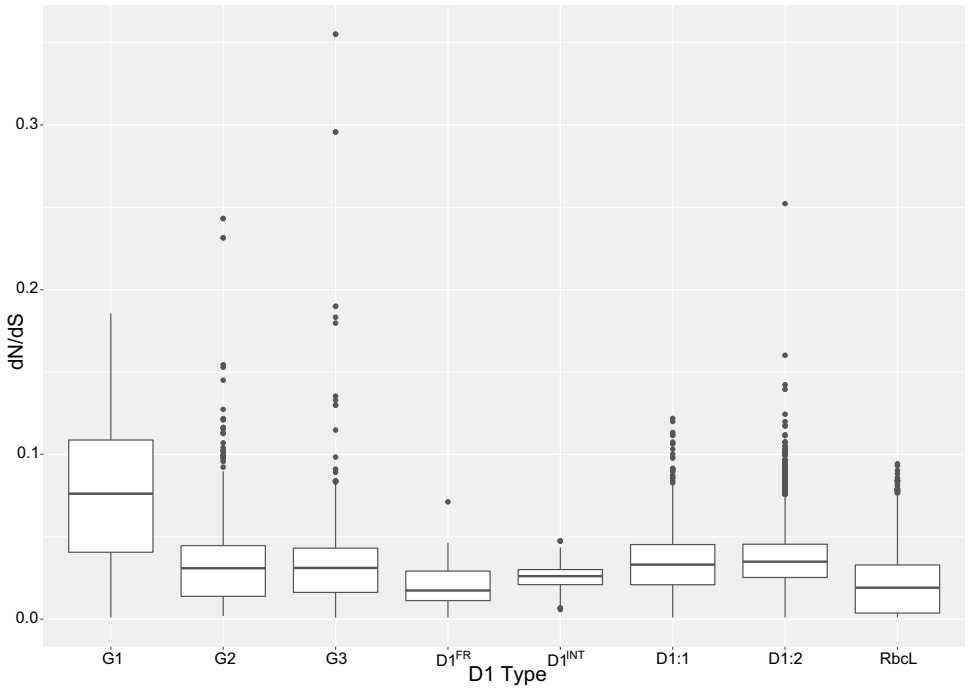

Fig. 6 Boxplot illustrating the range of ω (dN/dS) obtained by pairwise comparison of genes encoding for the proteins within each group of D1. Lines indicate the median and boxes delineate first and third quartiles, whiskers illustrate the minimum and maximum values and outliers are shown as individual points

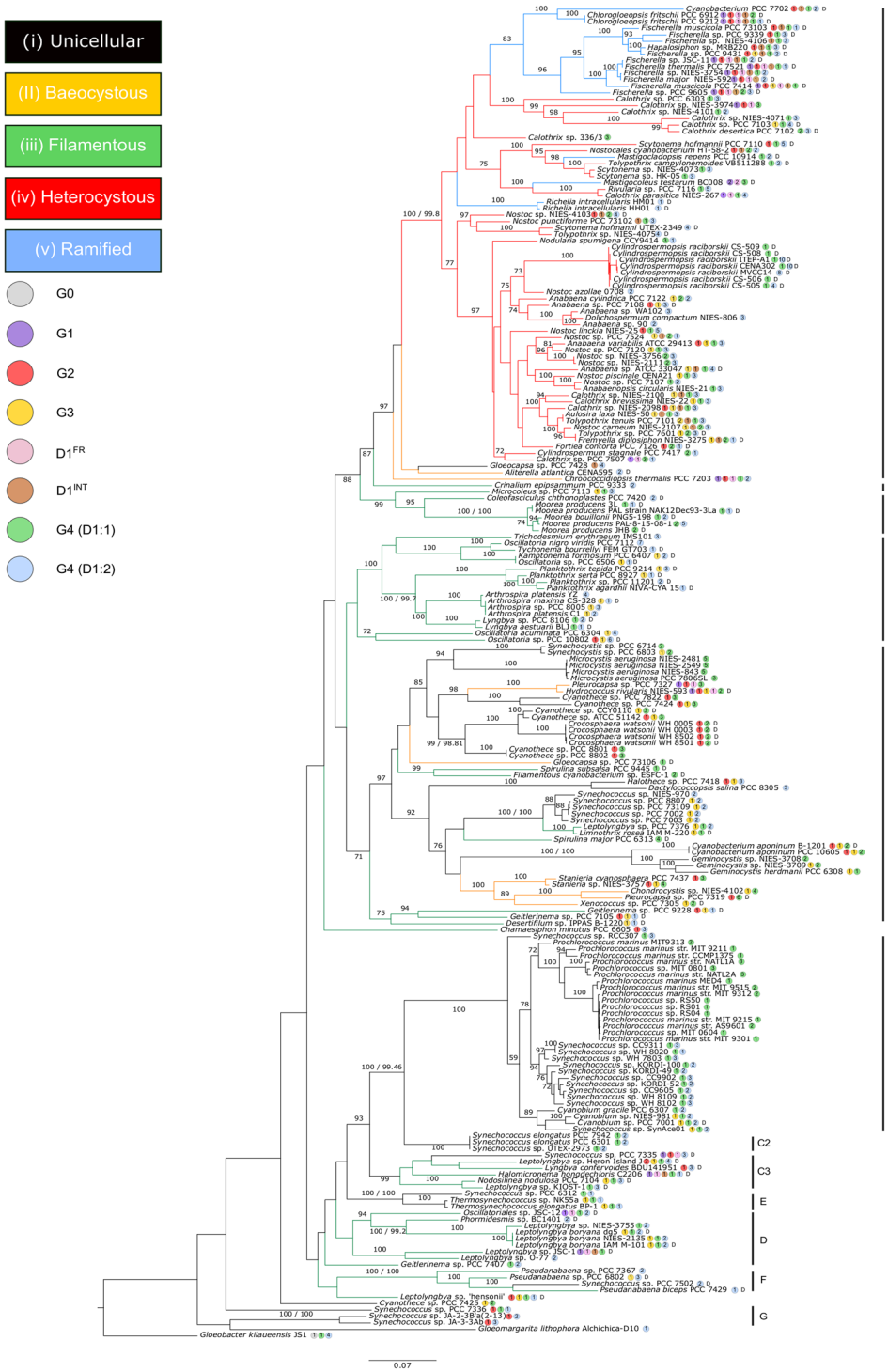

Fig. 7 Rooted maximum likelihood phylogeny of 16S–23S rRNA cyanobacterial sequences using *Gloeobacter kilaueensis* JS1 as the outgroup. Branch support over 70% from the maximum likelihood bootstrap are indicated, with branch support over 95% from the maximum parsimony tree also being highlighted (number of iterations = 1000). The D1 type and number of genes encoding each type that are present in each strain are indicated using coloured circles with G1, G2, G3, G4-D1:1 and G4-D1:2 protein sequences shown in purple, red, yellow, green and blue, respectively and the D1 proteins $D1^{FR}$ and $D1^{INT}$ are indicated in pink and brown, respectively. Phylogenetic subclades recovered in the Shih et al. (2013) analysis are indicated to the right of their corresponding groupings recovered in this analysis. A 'D' next to the D1 types for a strains indicates the data was obtained from a draft genome

cases updated genomes may vary (for example, in the contig assembly of *Fischerella* sp. PCC 9605, ALVT00000000, the $D1^{INT}$ was not identified, but it was present in the scaffold assembly of these contigs (KI912148–KI912154)).

The heterocystous cyanobacteria (subsection IV, Nostocales and subsection V, Stigonematales) form group B1 (Fig. 7). The majority of the Stigonematales formed a moderately supported subgroup within B1, these included cyanobacteria with *psbA* genes encoding the largest number of D1 types. Genes encoding $D1^{INT}$ and G2-D1 were very common in these strains and more than half had genes encoding G1-D1, G2-D1, G4-D1, $D1^{FR}$ and $D1^{INT}$, whereas only two strains had genes encoding G3-D1. The rest of the B1 subgroup were predominately Nostocales strains

and these had greater variation in *psbA* gene diversity. Only four of the 54 Nostocales strains in this analysis contained genes coding for G1-D1 and $D1^{FR}$ but genes encoding G2-D1, $D1^{INT}$ and G3-D1 where in 9, 10 and 16 strains, respectively. The B1 strains had between 1 and 11 *psbA* copies encoding G4-D1, this included the draft genomes of *Cylindrospermopsis raciborskii* strains CENA302 and ITEP-A1 which each had 11 copies. In addition, the draft genome of *Fischerella* sp. PCC 9605 had nine copies and the draft genomes of *C. raciborskii* MVCC14, *Leptolyngbya* Heron Island J and *Nostoc* NIES-403 each had eight copies of *psbA* encoding G4-D1. Several Nostocales strains (26 strains) had only genes coding for G4-D1, this included the obligate symbionts *Nostoc azollae* 0708, *Richelia intracellularis* HM01 and *Richelia intracellularis* HH01 and also free-living strains from marine, freshwater and terrestrial environments. Some of these strains contained only genes for D1:1 or D1:2, although most strains contained both.

There is a striking decrease in diversity of *psbA* genes in the filamentous non-heterocystous cyanobacteria in A1 and B2a groups compared to the heterocystous cyanobacteria. More than half of the A1 and B2a strains (14/24) contain only genes encoding G4-D1; in addition, genes encoding G3-D1 and G2-D1 were found in ten strains and one strain, respectively. Sister to these is a moderately supported group, B2b that contains unicellular and filamentous cyanobacteria, the majority (> 70%) of these strains have genes coding for at least two D1 types. Similar to groups A1 and B2a, the gene encoding G3-D1 is common, being present in half these strains; in contrast, many more of the strains (~ 40%) have genes encoding G2-D1 but only two strains have the FaRLiP gene cluster.

The well-supported group C1 includes members of the *Prochlorococcus* genus, these strains have contracted genomes relative to other cyanobacteria and inhabit the nutrient poor, oligotrophic oceans (Scanlan et al. 2009). This genus utilises a range of light-inducible proteins for photoprotection (Rocap et al. 2003), which may result in a reduced reliance on D1:2 to reduce the rates of photoinhibition, consistent with these strains having one to three copies of *psbA* encoding the G4-D1:1 protein (Mella-Flores et al. 2012). Sister to the *Prochlorococcus* subgroup is a well-supported subgroup of marine *Synechococcus* strains; these have genes encoding both G4 isoforms and sister to this is a smaller group containing four unicellular strains that each contain *psbA* genes encoding G3-D1. The C2 subgroup contains three *Synechococcus* strains with genes for both the G4-D1 proteins. In contrast, the well-supported subgroup C3 contains both unicellular and filamentous cyanobacteria and these exhibit variation in their *psbA* diversity, all containing genes for G4-D1 (both D1:1 and D1:2) and for up to three other D1 types, including two strains containing the FaRLiP cluster: *Synechococcus* sp. PCC 7335 and *Halomicronema hongdechloris* C2206. The subgroups E, D and F contain cyanobacteria with genes encoding G4-D1 alone or in combination with G3-D1 (14 strains), with the exception of two strains with the FaRLiP gene cluster (*Oscillatoriales cyanobacterium* JSC-12 and *Leptolyngbya* sp. JSC-1), one of which also has the gene encoding $D1^{INT}$ (*Leptolyngbya* sp. JSC-1). The hot-spring-inhabiting *Synechococcus* spp. JA-3-3Ab and JA-2-3B′a (2–13) (subgroup G, Fig. 7) are among the most deeply branching cyanobacteria identified (Shih et al. 2013; Li et al. 2014; Sánchez-Baracaldo et al. 2017; Moore et al. 2019) and have genes encoding G4-D1:2 and G2-D1.

Potential roles for the *psbA* gene family in cyanobacteria

The grouping of D1 proteins did not follow the topology of the 16S–23S rRNA gene phylogeny (Figs. 1, 7). The D1 phylogeny showed six groups of D1 proteins, and the 16S–23S rRNA phylogeny annotated with the distribution of the D1 protein types indicates the presence of the different D1 types in strains across the phylogeny. Well-supported groups of closely related strains tend to have similar D1 protein complements, suggesting different cyanobacterial lineages have retained and lost specific D1 types. More than half the strains (106/206) had at least one D1 type in addition to G4-D1, with ~ 30% and ~ 14% of all strains having one or two additional D1 types, respectively. Furthermore, ~ 8% of strains have three or more D1 types in addition to G4-D1. Out of the 100 strains with only G4-D1 proteins, 43 strains have genes encoding both D1:1 and D1:2 proteins, 31 have only D1:1 proteins and 26 have only D1:2 proteins. Only ~ 10% of the cyanobacterial strains had a single copy of *psbA* and it should be noted that many of these are draft genomes. We interpret the prevalence of different D1 types and multiple copies of the same D1 type in most cyanobacterial strains to be indicative of a selective advantage to maintaining these copies, although the function of some D1 types is not clear.

Microenvironments occupied by the cyanobacteria may have led to the retention of different D1 types: for example, Gan and Bryant (2015) suggested that the far-red-inducible gene cluster may confer an advantage when green light is either scattered or absorbed by the environment or competing photoautotrophic organisms are present. In our analysis, a phylogenetically diverse collection of cyanobacteria had the FaRLiP cluster and these were isolated from environments that had the potential to be competitive for light. For example, a niche for chlorophyll *f*-containing cyanobacteria was identified below the surface of a hot spring microbial mat where only wavelengths of light > 700 nm remained (Ohkubo and Miyashita 2017) and eleven strains with the FaRLiP cluster were isolated from hot springs. Two strains were isolated from associations with other phototrophs: one

as an endophyte of a red alga and one from a stromatolite. In addition, two strains were from soil and one from a sphagnum bog and all of these environments have potential to be far-"red-light" enriched (Gan and Bryant 2015).

The gene encoding the $D1^{INT}$ protein was found predominately in heterocystous cyanobacteria, but only in a third of heterocystous strain' genomes. Both Nostocales and Stigonematales strains contained the gene encoding $D1^{INT}$ along with three additional non-heterocystous strains. The three strains were the unicellular *Gloeocapsa* sp. PCC 7428, which also has four genes encoding D1:2 copies and was isolated from a hot spring, and the filamentous strains *Leptolyngbya* JSC-1 isolated from a hot spring and *Halomicronema hongdechloris* C2206 isolated from a stromatolite; both of these filamentous strains also have the FaRLiP cluster. The $D1^{INT}$ was found in a similar number of strains as the FaRLiP gene cluster. There was no clear pattern of co-occurrence with other *psbA* genes; however, 24 of the 27 strains had at least three D1 types.

The G3-D1 protein was in a phylogenetically broad range of cyanobacteria that represented about ~ 30% of the strains in this analysis. The gene encoding G3-D1 is up-regulated under low oxygen in several cyanobacterial strains (Summerfield et al. 2008; Sicora et al. 2009). Cardona et al. (2018) estimate the G3-D1 to have evolved around the time of the Great Oxidation Event branching slightly before G4-D1, raising the possibility that these genes evolved under low-oxygen conditions and were down-regulated in the presence of oxygen. This regulation has been demonstrated in a *Synechocystis* sp. PCC 6803 strain containing only the low-oxygen-expressed *psbA* gene (Summerfield et al. 2008; Crawford et al. 2016). The *psbA* genes encoding G3-D1 are under relatively strong purifying selection in both diazotrophic and non-diazotrophic strains indicating a current physiological function. Low-oxygen conditions are also associated with the up-regulation of genes encoding other components of the photosynthetic electron transport chain (Summerfield et al. 2008). In addition, under low oxygen G3-D1 PS II centres were less susceptible to photoinhibition than G4-D1 PS II centres in *Synechocystis* sp. PCC 6803 (Crawford et al. 2016).

The G2-D1 protein has been suggested to be involved in protecting nitrogenase in unicellular diazotrophs (Wegener et al. 2015). Of the strains analysed from the unicellular diazotrophs *Crocosphaera watsonii* and *Cyanothece* spp., most have genes encoding G2-D1 except *Cyanothece* sp. CCY 0110, for which only a draft genome was available and therefore data may be missing, and *Cyanothece* sp. PCC 7425 for which a complete genome was available. Unlike the other *Cyanothece* strains, *Cyanothece* sp. PCC 7425 is not an aerobic diazotroph and has been identified as belonging to the Synechococcales based on thylakoid structure and molecular phylogenetic analysis (Mares et al. 2019). The presence of G2-D1 in unicellular diazotrophs is consistent with subjective dark detection of low levels of G2-D1-containing PS II centres in *Crocosphaera watsonii* WH8501 (Masuda et al. 2018) and the suggestion G2-D1-containing PS II centres have a role in the temporal regulation of diazotrophy and photosynthesis (Wegener et al. 2015; Masuda et al. 2018; Sicora et al. 2019).

Genes encoding G2-D1 were identified in the genomes of heterocystous, filamentous non-heterocystous and unicellular strains: most of which have been demonstrated to be nitrogen fixing or have the *nif* gene cluster but a further seven strains had the G2-D1-encoding gene but did not have genes encoding nitrogenase. Strains containing *psbA* encoding G2-D1 were members of the orders: Chroococcales, Pleurocapsales, Chroococcidiopsidales, Synechococcales, Oscillatoriales, Nostocales and Stigonematales. The wide distribution of *psbA* encoding G2-D1 in strains that employ different strategies for separating photosynthesis and nitrogen fixation appears to indicate additional roles for G2-D1-containing PS II centres. In our analysis, 22 of the 71 heterocystous strains contained a gene coding for G2-D1, these strains would not require G2-D1 PS II centres to protect nitrogenase as PS II and nitrogenase would be spatially separated. Several unicellular and filamentous diazotrophs lack the gene, including *Xenococcus* sp. PCC 9228, *Pseudanabaena* sp. PCC 6802, *Microcoleus* sp. PCC 7113, *Trichodesmium erythraeum* IMS101 and *Lyngbya* sp. PCC 8106. The distribution of the gene encoding G2-D1 included absence from some non-heterocystous diazotrophs, and presence in some heterocystous strains and a small number of non-diazotrophic strains indicate additional or alternative roles of G2-D1. In total, a quarter of strains in our analysis had the *psbA* that encoded G2-D1 and it has been shown to be up-regulated in *Anabaena variabilis* ATCC 29413 in heterotrophically grown filaments (Park et al. 2013) consistent with a physiological role for this isoform.

We propose that all six different copies of D1 may confer selective advantages in specific microhabitats. Furthermore, carrying a large suite of D1 proteins might impart a competitive advantage in a fluctuating environment and may explain the diversity of D1 proteins in some cyanobacterial strains.

Conclusion

Our analysis of the D1 family members and their distribution in cyanobacteria has identified a phylogenetically distinct D1 group; this contains two subgroups: $D1^{FR}$ and $D1^{INT}$. The genes encoding these proteins were under similar selective pressure to the genes encoding other types of D1. The $D1^{INT}$ protein has the ligands necessary to bind the OEC and was found in a phylogenetically diverse range of cyanobacteria but predominantly in heterocystous cyanobacteria

and this was in about one-third of the heterocystous strains. The gene encoding the $D1^{FR}$ protein was part of the FaRLiP cluster, which also contains a gene encoding the enzymatic form of D1 — the G1, chlorophyll *f* synthase. The $D1^{FR}$ protein has the ligands necessary to bind the OEC and several amino acid changes that might be associated with binding of chlorophyll *f*, rather than chlorophyll *a*, consistent with its involvement in the far-red light acclimation process. Furthermore, the previously identified G3-D1 group was shown to contain three subgroups. Subgroup I had changes predominately towards the N-terminus of the D1 protein, whereas subgroup III had most variation from the G4 consensus towards the C-terminus. In this analysis, ~ 30% of cyanobacteria contained a gene encoding one of these two G3-D1 subgroups.

The gene encoding G2-D1 was found in 25% of cyanobacteria, many of which, but not all, are diazotrophic strains. However, many diazotrophic strains (both unicellular and filamentous) do not contain genes encoding G2-D1. Each group of D1 proteins was found in a phylogenetically diverse range of cyanobacteria consistent with ancestral cyanobacteria having multiple copies of D1. The filamentous heterocystous cyanobacteria tended to have more D1 types, perhaps reflecting an enhanced capacity to adapt to changing environmental conditions. These analyses support the idea that distinct D1 types confer a selective advantage under specific conditions that has led to their retention in a phylogenetically diverse range of cyanobacteria.

Additional information

The data reported in this paper have come from genomes deposited in both the Genbank and JGI databases (accession nos. CP000117, CP000393, CP003614, CP003620, CP003642, CP006269, CP006270, CP006271, CP006471, CP006882, CP007203, CP007542, CP007753, CP007754, CP011304, CP011382, CP011456, CP011941, CP012036, CP012375, CP013008, CP013998, CP016474, CP016483, CP017599, CP017675, CP017708, CP018091, CP018344, CP018345, CP018346, CP019636, CP020771, CP021983, FO818640, Ga0010025, Ga0012361, Ga0012362, Ga0014323, Ga0025054, Ga0025357, Ga0025386, Ga0025408, Ga0026686, Ga0064116, Ga0064117, Ga0078583, Ga0079976, Ga0166459, NC_003272, NC_004113, NC_005042, NC_005070, NC_005071, NC_005072, NC_006576, NC_007335, NC_007513, NC_007516, NC_007577, NC_007604, NC_007775, NC_007776, NC_008319, NC_008816, NC_008817, NC_008819, NC_009091, NC_009481, NC_009482, NC_009840, NC_009976, NC_010296, NC_010475, NC_010546, NC_010628, NC_011726, NC_011729, NC_011884, NC_013161, NC_014248, NC_014501, NC_019427, NC_019675, NC_019676, NC_019678, NC_019680, NC_019682, NC_019683, NC_019684, NC_019689, NC_019693, NC_019695, NC_019697, NC_019701, NC_019702, NC_019703, NC_019738, NC_019745, NC_019748, NC_019751, NC_019771, NC_019776, NC_019779, NC_019780, NC_020286, NC_022600, NC_023033, AAVU00000000, AAXW00000000, ABRV00000000, ABRS00000000, ABSE00000000, ABYK00000000, ACYA00000000, AGCR00000000, AGIZ00000000, AJLJ00000000, AJLK00000000, AJLL00000000, AJLM00000000, AJLN00000000, AJWF00000000, ALVI00000000, ALVJ00000000, ALVK00000000, ALVL00000000, ALVP00000000, ALVQ00000000, ALVR00000000, ALVS00000000, ALVT00000000, ALVW00000000, ALVX00000000, ALVY00000000, ALVZ00000000, ALWB00000000, ALWD00000000, ANFJ00000000, ANFQ00000000, ANNX00000000, AP014638, AP014642, AP014815, AP014821, AP017295, AP017308, AP017367, AP017375, AP017959, AP018172, AP018174, AP018178, AP018180, AP018184, AP018194, AP018203, AP018207, AP018222, AP018227, AP018233, AP018248, AP018254, AP018255, AP018268, AP018280, AP018281, AP018288, AP018298, AP018307, AP018316, AP017305, AUZM00000000, AVFS00000000, AWNH00000000, BDUC00000000, CACA00000000, CAIS00000000, CAIY00000000, CM001632, CM001775, CM001776, CZCT00000000, CZCU00000000, CZDF00000000, JMKF00000000, JQFA00000000, JTHE00000000, JXCB00000000, JYON00000000, LIRN00000000, LMTZ00000000, LNDC00000000, LT578417, LUBZ00000000, LUHI00000000, MBQX00000000, MBQY00000000, MKZR00000000, MKZS00000000, MQTZ00000000, MRBY00000000, MRCA00000000, MRCB00000000, MTPU00000000, NXIB00000000, PEBC00000000).

Acknowledgements The authors would like to acknowledge Andy Nilsen for the valuable discussions while creating the phylogenetic trees and Bronwyn Carlisle for helping to finalise the figures for publication. KJS is supported by a University of Otago Division of Sciences PhD Scholarship. Additional funding was provided by a University of Otago research grant to TCS.

Compliance with ethical standards

Conflict of interest The authors declare that they have no conflict of interest.

References

Ago H, Adachi H, Umena Y, Tashiro T, Kawakami K, Kamiya N, Tian L, Han G, Kuang T, Liu Z, Wang F, Zou H, Enami I, Miyano M, Shen JR (2016) Novel features of eukaryotic

Photosystem II revealed by its crystal structure analysis from a red alga. J Biol Chem 291:5676–5687. https://doi.org/10.1074/jbcM115.711689

Banerjee G, Ghosh I, Kim CJ, Debus RJ, Brudvig GW (2018) Substitution of the D1-Asn87 site in Photosystem II of cyanobacteria mimics the chloride-binding characteristics of spinach Photosystem II. J Biol Chem 293:2487–2497. https://doi.org/10.1074/jbc.M117.813170

Banerjee G, Ghosh I, Kim CJ, Debus RJ, Brudvig GW (2019) Bicarbonate rescues damaged proton-transfer pathway in Photosystem II. BBA Bioenerg 1860:611–617. https://doi.org/10.1016/j.bbabio.2019.06.014

Benson DA, Cavanaug M, Clark K, Karsch-Mizrachi I, Lipman DJ, Ostell J, Sayers EW (2017) Genbank. Nucleic Acids Res 45:37–42. https://doi.org/10.1093/nar/gks1195

Bertoni M, Kiefer F, Biasini M, Bordoli L, Schwede T (2017) Modeling protein quaternary structure of homo- and hetero-oligomers beyond binary interactions by homology. Sci Rep 7:10480. https://doi.org/10.1038/s41598-017-09654-8

Bienert S, Waterhouse A, de Beer TAP, Tauriello G, Studer G, Bordoli L, Schwede T (2017) The SWISS-MODEL Repository - new features and functionality. Nucleic Acids Res 45:313–319. https://doi.org/10.1093/nar/gkw1132

Cardona T, Sedoud A, Cox N, Rutherford AW (2012) Charge separation in photosystem II: a comparative and evolutionary overview. BBA Bioenerg 1817:26–43. https://doi.org/10.1016/j.bbabio.2011.07.012

Cardona T, Murray JW, Rutherford AW (2015) Origin and evolution of water oxidation before the last common ancestor of the cyanobacteria. Mol Biol Evol 32:1310–1328. https://doi.org/10.1093/molbev/msv024

Cardona T, Sánchez-Baracaldo P, Rutherford AW, Larkum AWD (2019) Early archean origin of photosystem II. Geobiology 17:127–150

Chen M, Schliep M, Willows RD, Cai ZL, Neilan BA, Scheer H (2010) A red-shifted chlorophyll. Science 329:1318–1319. https://doi.org/10.1126/science.1191127

Chen M, Li Y, Birch D, Willows RD (2012) A cyanobacterium that contains chlorophyll *f* – a red-absorbing photopigment. FEBS Lett 586:3249–3254. https://doi.org/10.1016/j.febslet.2012.06.045

Chen M, Hernandez-Prieto MA, Loughlin PC, Li Y, Willows RD (2019) Genome and proteome of the chlorophyll *f*-producing cyanobacterium *Halomicronema hongdechloris*: adaptative proteomic shifts under different light conditions. BMC Genomics 20:207. https://doi.org/10.1186/s12864-019-5587-3

Crawford TS, Hanning KR, Chua JP, Eaton-Rye JJ, Summerfield TC (2016) Comparison of D1′- and D1-containing PS II reaction centre complexes under different environmental conditions in *Synechocystis* sp. PCC 6803. Plant Cell Environ 39:1715–1726. https://doi.org/10.1111/pce.12738

Darriba D, Taboada GL, Doallo R, Posada D (2012) jModelTest 2 more models new heuristics and parallel computing. Nat Methods 9:772. https://doi.org/10.1038/nmeth.2109

DeLano WL (2002) Pymol: an open-source molecular graphics tool. CCP4 newsletter on protein. Crystallography 40:82–92

DeLano WL (2009) PyMOL molecular viewer Updates and refinements. In: Abstracts of Papers of the American Chemical Society (Vol. 238). American Chemical Society, Washington DC.

El Bissati K, Kirilovsky D (2001) Regulation of *psbA* and *psaE* expression by light quality in *Synechocystis* species PCC 6803. A redox control mechanism. Plant Physiol 125:1988–2000. https://doi.org/10.1104/pp.125.4.1988

Endo K, Kobayashi K, Wang H-T, Chu H-A, Shen J-R, Wada H (2019) Site-directed mutagenesis of two amino acid residues in cytochrome b_{559} α subunit that interact with a phosphatidylglycerol molecule (PG772) induces quinone-dependent inhibition of Photosystem II activity. Photosynth Res 139:267–279. https://doi.org/10.1007/s11120-018-0555-3

Felsenstein J (1985) Confidence limits on phylogenies: an approach using the bootstrap. Evolution 39:783–791. https://doi.org/10.1111/j.1558-5646.1985.tb00420.x

Ferreira KN, Iverson TM, Maghlaoui K, Barber J, Iwata S (2004) Architecture of the photosynthetic oxygen-evolving center. Science 303:1831–1838. https://doi.org/10.1126/science.1093087

Fletcher W, Yang Z (2010) The effect of insertions deletions and alignment errors on the branch-site test of positive selection. Mol Biol Evol 27:2257–2267. https://doi.org/10.1093/molbev/msq115

Funk C, Wiklund R, Schröder WP, Jansson C (2001) D1′ centers are less efficient than normal photosystem II centers. FEBS Lett 505:113–117. https://doi.org/10.1016/S0014-5793(01)02794-6

Gan F, Bryant DA (2015) Adaptive and acclimative responses of cyanobacteria to far-red light. Environ Microbiol 17:3450–3465. https://doi.org/10.1111/1462-2920.12992

Gan F, Zhang S, Rockwell NC, Martin SS, Lagarias JC, Bryant DA (2014) Extensive remodeling of a cyanobacterial photosynthetic apparatus in far-red light. Science 345:1312–1317. https://doi.org/10.1126/science.1256963

Gan F, Shen G, Bryant DA (2015) Occurrence of far-red light photoacclimation (FaRLiP) in diverse cyanobacteria. Life 5:4–24. https://doi.org/10.3390/life5010004

Grigoriev IV, Nordberg H, Shabalov I, Aerts A, Cantor M, Goodstein D, Kuo A, Minovitsky S, Nikitin R, Ohm RA, Otillar R, Poliakov A, Ratnere I, Riley R, Smirnova T, Rokhsar D, Dubchak I (2012) The genome portal of the department of energy joint genome institute. Nucleic Acids Res 40:26–32. https://doi.org/10.1093/nar/gkt1069

Grim SL, Dick GJ (2016) Photosynthetic versatilityin the genome of *Geitlerinema* sp. PCC 9228 (Formerly *Oscillatoria limnetica* 'Solar Lake'), a model anoxygenic photosynthetic cyanobacterium. Front Microbiol 7:26–32. https://doi.org/10.3389/fmicb.2016.01546

Guex N, Peitsch MC, Schwede T (2009) Automated comparative protein structure modeling with SWISS-MODEL and Swiss-PdbViewer A historical perspective. Electrophoresis 30:162–173. https://doi.org/10.1002/elps.200900140

Hakovirta JR, Prezioso S, Hodge D, Pillai SP, Weigel LM (2016) Identification and analysis of informative single nucleotide polymorphisms in 16S rRNA gene sequences of the *Bacillus cereus* group. J Clin Microbiol 54:2749–2756. https://doi.org/10.1128/JCM.01267-16

Hilton JA, Meeks JC, Zehr JP (2016) Surveying DNA Elements within functional genes of heterocyst-forming cyanobacteria. PLoS ONE 11:e0156034. https://doi.org/10.1371/journal.pone.0156034

Ho MY, Bryant DA (2019) Global transcriptional profiling of the cyanobacterium *Chlorogloeopsis fritschii* PCC 9212 in far-red light insights into the regulation of chlorophyll *d* synthesis. Front Microbiol 10:465. https://doi.org/10.3389/fmicb.2019.00465

Ho MY, Shen G, Canniffe DP, Zhao C, Bryant DA (2016) Light-dependent chlorophyll *f* synthase is a highly divergent paralog of PsbA of Photosystem II. Science 353:aff9178. https://doi.org/10.1126/science.aaf9178

Ho MY, Niedzwiedzki DM, MacGregor-Chatwin C, Gerstenecker G, Hunter CN, Blankenship RE, Bryant DA (2019) Extensive remodeling of the photosynthetic apparatus alters energy transfer among photosynthetic complexes when cyanobacteria acclimate to far-red light. BBA Bioenerg. https://doi.org/10.1016/j.bbabio.2019.148064

Hongo JA, Castro GM, Cintra LC, Zerlotini A, Lobo FP (2015) POTION an end-to-end pipeline for positive Darwinian selection detection in genome-scale data through phylogenetic comparison of protein-coding genes. BMC Genomics 16:567. https://doi.org/10.1186/s12864-015-1765-0

Jaspers E, Overmann J (2004) Ecological significance of microdiversity: identical 16S rRNA gene sequences can be found in bacteria with highly divergent genomes and ecophysiologies. Appl Environ Microbiol 70:4831–4839. https://doi.org/10.1128/AEM.70.8.4831-4839.2004

Kern J, Biesiadka J, Loll B, Saenger W, Zouni A (2007) Structure of the Mn_4-Ca cluster as derived from X-ray diffraction. Photosynth Res 92:389–405. https://doi.org/10.1007/s11120-007-9173-1

Kern J, Chatterjee R, Young ID et al (2018) Structures of the intermediates of Kok's photosynthetic water oxidation clock. Nature 563:421–425. https://doi.org/10.1038/s41586-018-0681-2

Larkin MA, Blackshields G, Brown NP, Chenna R, McGettigan PA, McWilliam H, Valentin F, Wallace IM, Wilm A, Lopez R, Thompson JD (2007) Clustal W and Clustal X version 2.0. Bioinformatics 23:2947–2948. https://doi.org/10.1093/bioinformatics/btm404

Le SQ, Gascuel O (2008) An improved general amino acid replacement matrix. Mol Biol Evol 25:1307–1320. https://doi.org/10.1093/molbev/msn067

Li B, Lopes JS, Foster PG, Embley TM, Cox CJ (2014) Compositional biases among synonymous substitutions cause conflict between gene and protein trees for plastid origins. Mol Biol Evol 31:1697–1709. https://doi.org/10.1093/molbev/msu105

Mares J, Johansen JR, Hauer T, Zima J Jr, Ventura S, Cuzman O, Tiribilli B, Kastovsky J (2019) Taxonomic resolution of the genus *Cyanothece* (Chroococcales, Cyanobacteria), with a treatment on *Gloeothece* and three new genera, *Crocosphaera, Rippkaea*, and *Zehria*. J Phycol 55:578–610. https://doi.org/10.1111/jpy.12853

Masuda T, Bernát G, Bečková M, Kotabová E, Lawrenz E, Lukeš M, Komenda J, Prášil O (2018) Diel regulation of photosynthetic activity in the oceanic unicellular diazotrophic cyanobacterium *Crocosphaera watsonii* WH8501. Environ Microbiol 20:546–560. https://doi.org/10.1111/1462-2920.13963

Mella-Flores D, Six C, Ratin M, Partensky F, Boutte C, Le Corguillé G, Blot N, Gourvil P, Kolowrat C, Garczarek L, Marie D (2012) *Prochlorococcus* and *Synechococcus* have evolved different adaptive mechanisms to cope with light and UV stress. Front Microbiol 3:285. https://doi.org/10.3389/fmicb.2012.00285

Moore KR, Magnabosco C, Momper L, Gold DA, Bosak T, Fournier GP (2019) An expanded ribosomal phylogeny of cyanobacteria supports a deep placement of plastids. Front Microbiol 10:1612. https://doi.org/10.3389/fmicb.2019.01612

Mulo P, Sicora C, Aro EM (2009) Cyanobacterial *psbA* gene family optimization of oxygenic photosynthesis. Cell Mol Life Sci 66:3697. https://doi.org/10.1007/s00018-009-0103-6

Mulo P, Sakurai I, Aro EM (2012) Strategies for *psbA* gene expression in cyanobacteria green algae and higher plants from transcription to PSII repair. BBA Bioenerg 1817:247–257. https://doi.org/10.1016/j.bbabio.2011.04.011

Murray JW (2012) Sequence variation at the oxygen-evolving centre of Photosystem II a new class of 'rogue' cyanobacterial D1 proteins. Photosynth Res 110:177–184. https://doi.org/10.1007/s11120-011-9714-5

Narusaka Y, Murakami A, Saeki M, Kobayashi H, Satoh K (1996) Preliminary characterization of a photo-tolerant mutant of *Synechocystis* sp. PCC 6803 obtained by in vitro random mutagenesis of *psbA2*. Plant Sci 115:261–266. https://doi.org/10.1016/0168-9452(96)04393-2

Narusaka Y, Narusaka M, Satoh K, Kobayashi H (1999) In vitro random mutagenesis of the D1 protein of the Photosystem II reaction center confers phototolerance on the cyanobacterium *Synechocystis* sp. PCC 6803. J Biol Chem 274:23270–23275. https://doi.org/10.1074/jbc.274.33.23270

Nordberg H, Cantor M, Dusheyko S, Hua S, Polakov A, Shabalov I, Smirnova T, Grigorie IV, Dubchak I (2014) The genome portal of the department of energy joint genome institute 2014 updates. Nucleic Acids Res 42:26–31. https://doi.org/10.1093/nar/gkt1069

Nürnberg DJ, Morton J, Santabarbara S, Telfer A, Joliot P, Antonaru LA, Ruban AV, Cardona T, Krausz E, Boussac A, Fantuzzi A, Rutherford AW (2018) Photochemistry beyond the red limit in chlorophyll *f*–containing photosystems. Science 360:1210–1213. https://doi.org/10.1126/science.aar8313

Ohkubo S, Miyashita H (2017) A niche for cyanobacteria producing chlorophyll f within a microbial mat. ISME J 11:2368–2378. https://doi.org/10.1038/ismej.2017.98

Park J-J, Lechno-Yossef S, Wolk CP, Vieille C (2013) Cell-specific gene expression in *Anabaena variabilis* grown phototrophically, mixotrophically, and heterotrophically. BMC Genomics 14:759. https://doi.org/10.1186/1471-2164-14-759

Partensky F, Six C, Ratin M, Garczarek L, Vaulot D, Probert I, Calteau A, Gourvil P, Marie D, Grébert T, Bouchier C (2018) A novel species of the marine cyanobacterium *Acaryochloris* with a unique pigment content and lifestyle. Sci Rep 8:9142. https://doi.org/10.1038/s41598-018-27542-7

Ponce-Toledo RI, Deschamps P, López-García P, Zivanovic Y, Benzerara K, David MD (2017) An Early-Branching Freshwater Cyanobacterium at the origin of plastids. Curr Biol 27:386–391. https://doi.org/10.1016/j.cub.2016.11.056

Quast C, Pruesse E, Yilmaz P, Gerken J, Schweer T, Yarza P, Peplies J, Glockner FO (2013) The SILVA ribosomal RNA gene database project improved data processing and web-based tools. Nucleic Acids Res 41:590–596. https://doi.org/10.1093/nar/gks1219

Rocap G, Larimer FW, Lamerdin J, Malfatti S, Chain P, Ahlgren NA, Arellano A, Coleman M, Hauser L, Hess WR, Johnson ZI (2003) Genome divergence in two *Prochlorococcus* ecotypes reflects oceanic niche differentiation. Nature 424:1042. https://doi.org/10.1038/nature01947

Sánchez-Baracaldo P, Raven JA, Pisani D, Knoll AH (2017) Early photosynthetic eukaryotes inhabited low-salinity habitats. Proc Natl Acad Sci USA 114:7737–7745. https://doi.org/10.1073/pnas.1620089114

Saw JH, Schatz M, Brown MV, Kunkel DD, Foster JS, Shick H, Christensen S, Hou S, Wan X, Donachie SP (2013) Cultivation and complete genome sequencing of Gloeobacter kilaueensis sp nov, from a lava cave in Kīlauea Caldera Hawai'i. PLoS ONE 8:e76376. https://doi.org/10.1371/journal.pone.0076376

Scanlan DJ, Ostrowski M, Mazard S, Dufresne A, Garczarek L, Hess WR, Post AF, Hagemann M, Paulsen I, Partensky F (2009) Ecological genomics of marine picocyanobacteria. Microbiol Mol Biol R 73:249–299. https://doi.org/10.1128/MMBR.00035-08

Shen J-R (2015) The structure of Photosystem II and the mechanism of water oxidation in photosynthesis. Annu Rev Plant Biol 66:23–48. https://doi.org/10.1146/annurev-arplant-050312-120129

Shen G, Canniffe DP, Ho MY, Kurashov V, van der Est A, Golbeck JH, Bryant DA (2019) Characterization of chlorophyll *f* synthase heterologously produced in *Synechococcus* sp. PCC 7002. Photosynth Res 140:1–16. https://doi.org/10.1007/s11120-018-00610-9

Shih PM, Wu D, Latifi A, Axen SD, Fewer DP, Talla E, Calteau A, Cai F, De Marsac NT, Rippka R, Herdman M (2013) Improving the coverage of the cyanobacterial phylum using diversity-driven genome sequencing. Proc Natl Acad Sci USA 110:1053–1058. https://doi.org/10.1073/pnas.1217107110

Shimodaira H, Hasegawa M (1999) Multiple comparisons of log-likelihoods with applications to phylogenetic inference. Mol Biol Evol 16:1114–1116. https://doi.org/10.1093/oxfordjournals.molbev.a026201

Shindyalov IN, Bourne PE (1998) Protein structure alignment by incremental combinatorial extension (CE) of the optimal path. Prot Eng 11:739–747. https://doi.org/10.1093/protein/11.9.739

Sicora C, Wiklund R, Jansson C, Vass I (2004) Charge stabilization and recombination in photosystem II containing the D1′ protein product of the psbAI gene in Synechocystis 6803. Phys Chem Chem Phys 6:4832–4837

Sicora C, Ho FM, Salminen T, Styring S, Aro EM (2009) Transcription of a "silent" cyanobacterial *psbA* gene is induced by microaerobic conditions. BBA Bioenerg 1787:105–112. https://doi.org/10.1016/j.bbabio.2008.12.002

Sicora CI, Chiş I, Chiş C, Sicora O (2019) Regulation of PSII function in *Cyanothece* sp. ATCC 51142 during a light–dark cycle. Photosynth Res 139:461–473. https://doi.org/10.1007/s11120-018-0598-5

Stamatakis A (2006) RAxML-VI-HPC maximum likelihood-based phylogenetic analyses with thousands of taxa and mixed models. Bioinformatics 22:2688–2690. https://doi.org/10.1093/bioinformatics/btl446

Suga M, Akita F, Hirata K, Ueno G, Murakami H, Nakajima Y, Shimizu T, Yamashita K, Yamamoto M, Ago H, Shen JR (2015) Native structure of Photosystem II at 1.95 Å resolution viewed by femtosecond X-ray pulses. Nature 517:99–103. https://doi.org/10.1038/nature13991

Suga M, Akita F, Sugahara M et al (2017) Light-induced structural changes and the site of O=O bond formation in PS II caught by XFEL. Nature 543:131–135. https://doi.org/10.1038/nature21400

Sugiura M, Ozaki Y, Nakamura M, Cox N, Rappaport F, Boussac A (2014) The D1–173 amino acid is a structural determinant of the critical interaction between D1-Tyr161 (TyrZ) and D1-His190 in Photosystem II. BBA Bioenerg 1837:1922–1931. https://doi.org/10.1016/j.bbabio.2014.08.008

Summerfield TC, Toepel J, Sherman LA (2008) Low-oxygen induction of normally cryptic *psbA* genes in cyanobacteria. Biochemistry 47:12939–12941. https://doi.org/10.1021/bi8018916

Swofford DL (2001) Paup*: Phylogenetic analysis using parsimony (and other methods) 4.0. B5.

Toepel J, Welsh E, Summerfield TC, Pakrasi HB, Sherman LA (2008) Differential transcriptional analysis of the cyanobacterium *Cyanothece* sp. strain ATCC 51142 during light-dark and continuous-light growth. J Bacteriol 190:3904–3913. https://doi.org/10.1128/JB.00206-08

Umena Y, Kawakami K, Shen JR, Kamiya N (2011) Crystal structure of oxygen-evolving Photosystem II at a resolution of 1.9 Å. Nature 473:55–60. https://doi.org/10.1038/nature09913

Vinyard DJ, Brudvig GW (2018) Progress toward a molecular mechanism of water oxidation in Photosystem II. Annu Rev Phys Chem 68:101–116. https://doi.org/10.1146/annurev-physchem-052516-044820

Vinyard DJ, Gimpel J, Ananyev GM, Mayfield SP, Dismukes GC (2014) Engineered Photosystem II reaction centers optimize photochemistry versus photoprotection at different solar intensities. J Am Chem Soc 136:4048–4055. https://doi.org/10.1021/ja5002967

Wada H, Murata N (2007) The essential role of phosphatidylglycerol in photosynthesis. Photosynth Res 92:205–215. https://doi.org/10.1007/s11120-007-9203-z

Waterhouse A, Bertoni M, Bienert S, Studer G, Tauriello G, Gumienny R, Heer FT, de Beer TAP, Rempfer C, Bordoli L, Lepore R, Schwede T (2018) SWISS-MODEL: homology modelling of protein structures and complexes. Nucleic Acids Res 46:296–303. https://doi.org/10.1093/nar/gky427

Wegener KM, Nagarajan A, Pakrasi HB (2015) An atypical *psbA* gene encodes a sentinel D1 protein to form a physiologically relevant inactive Photosystem II complex in cyanobacteria. J Biol Chem 290:3764–3774. https://doi.org/10.1074/jbc.M114.604124

Wei X, Su X, Cao P et al (2016) Structure of spinach Photosystem II – LHCII supercomplex at 3.2 Å resolution. Nature 534:69–74

Wiklund R, Salih GF, Mäenpää P, Jansson C (2001) Engineering of the protein environment around the redox-active TyrZ in Photosystem II. The role of F186 and P162 in the D1 protein of *Synechocystis* 6803. Eur J Biochem 268:5356–5364. https://doi.org/10.1046/j.0014-2956.2001.02466.x

Xu B, Yang Z (2013) PAMLX a graphical user interface for PAML. Mol Biol Evol 30:2723–2724. https://doi.org/10.1093/molbev/mst179

Yamasato A, Kamada T, Satoh K (2002) Random mutagenesis targeted to the *psbA*II gene of *Synechocystis* sp. PCC 6803 to identify functionally important residues in the D1 protein of the Photosystem II reaction center. Plant Cell Physiol 43:540–548. https://doi.org/10.1093/pcp/pcf066

Yang Z (2007) PAML 4 phylogenetic analysis by maximum likelihood. Mol Biol Evol 24:1586–1591. https://doi.org/10.1093/molbev/msm088

Zabelin AA, Shkuropatova VA, Makhneva ZK, Moskalenko AA, Shuvalov VA, Shkuropatov AY (2014) Chemically modified reaction centers of Photosystem II: Exchange of pheophytin a with 7-deformyl-7-hydroxymethyl-pheophytin b. BBA Bioenerg 1837:1870–1881. https://doi.org/10.1016/j.bbabio.2014.08.004